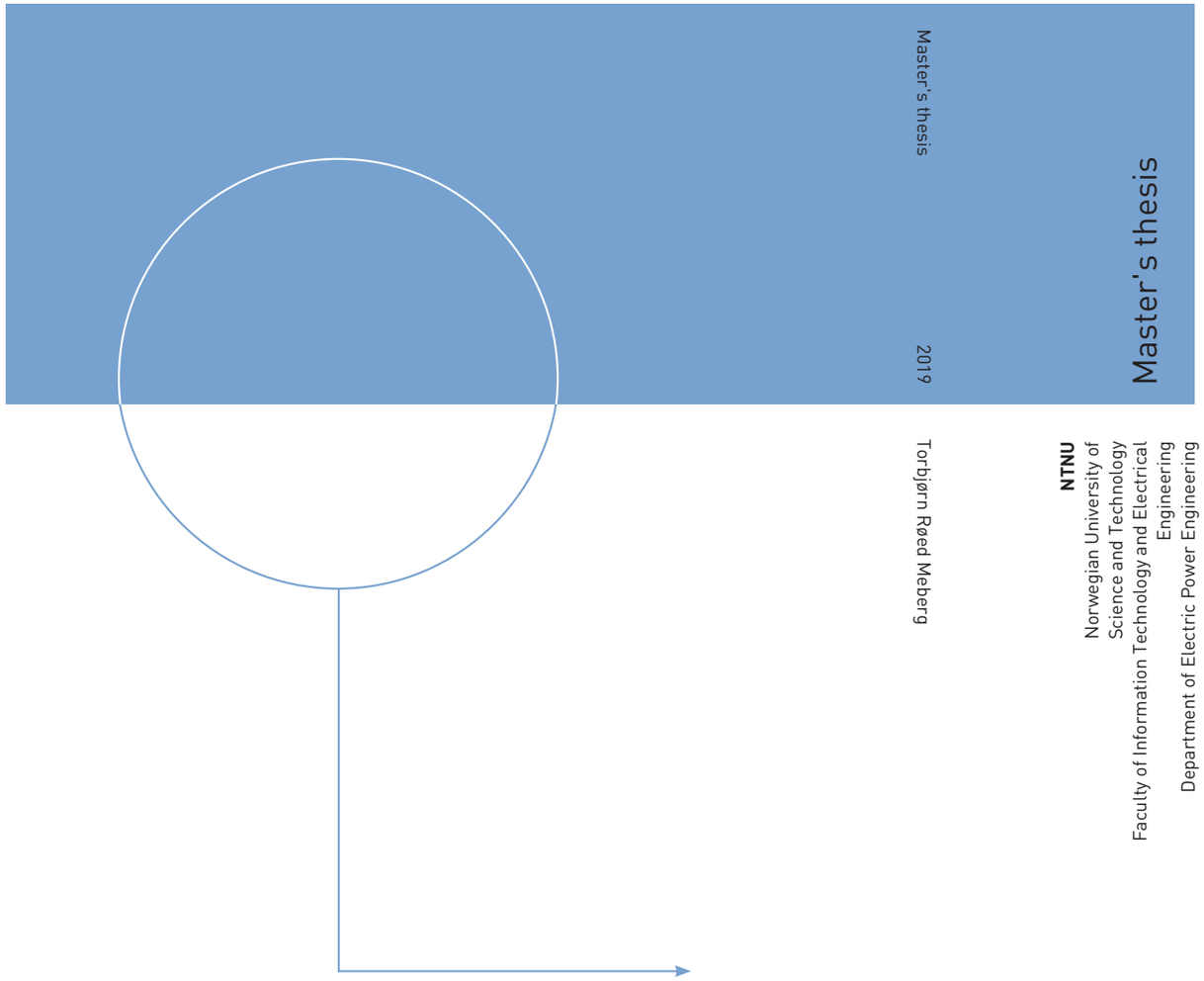

Master's thesis

2019

Torbjørn Røed Meberg

NTNU
Norwegian University of Science and Technology
Faculty of Information Technology and Electrical Engineering
Department of Electric Power Engineering

Torbjørn Røed Meberg

Flow-Based Market Coupling in Short-Term Hydro-Thermal Scheduling

June 2019

NTNU
Norwegian University of Science and Technology

NTNU
Norwegian University of Science and Technology

NTNU

Norwegian University of
Science and Technology

Flow-Based Market Coupling in Short-Term Hydro-Thermal Scheduling

Torbjørn Røed Meberg

Energy and Environmental Engineering
Submission date: June 2019
Supervisor: Arild Helseth
Co-supervisor: Hossein Farahmand
Christian Øyn Naversen

Norwegian University of Science and Technology
Department of Electric Power Engineering

Abstract

The utilization of the power grid is under transition, where an increase in generation from renewable energy sources combined with electrification of the industry, changes the composition of the grid. The current grid is not designed for the stress that these changes inflict, thus forcing the transmission system operator to upgrade the grid. Flow-based market coupling provides a greater utilization of the physical limits of the grid, thus increasing the flexibility and socio-economic benefits. The cross-zonal trading will be closer to the physical flow with FBMC, than the conventional ATC market coupling [41].

To overcome the uncertainties related to the change in the power system composition, SINTEF Energy Research is developing a short-term fundamental multi-market model to enumerate the products in the electricity market, to better the investment analysis of the upgrading and building of new cables and plants.

The master thesis is performed with the goal to contribute to the model, PriMod, by implementing flow-based market coupling, to increase its accuracy of simulations in the future power system. Moreover, the thesis analyses how the implementation is affecting the simulations, both in terms of flow of power and how it is coupled with the prices.

The results from the simulation shows promising results in an economic perspective. When compared to the original model, the simulation with

flow-based market coupling shows that in addition to lower average and median prices, it also leads to a higher level of converging prices. Further it can be argued that the method may decrease the level of congestion in the grid, as the power follows its physical characteristics to a higher extent. Apart from the solely positive results, the significant amount of occurrences of ”non-intuitive” power flows, is discussed. In a flow-based market, this concept needs to be considered by the producers, as the power may flow to a lower priced area, thus reducing their profits. Last, suggestions of how the model could be expanded and improved are presented and discussed, to increase accuracy and to model interesting aspects of the power market.

Sammendrag

Flyten av kraft i det nordiske kraftsystemet er under endring, der det er en økning i produksjon fra fornybare energikilder i tillegg til en elektrifisering av ulike deler av industrisektoren, som forandrer sammensetningen i kraftnettet. Det nåværende kraftsystemet er ikke designet for den økende påkjenningen fra disse endringene, som fører til at systemoperatøren er nødt til å foreta oppgraderinger av nettet. Flytbasert markedskobling gir muligheten for en høyere utnyttelsesgrad av kapasiteten i nettet, og gir således mer fleksibilitet og høyere sosio-økonomisk overskudd. Flyt av kraft mellom soner vil ligge nærmere den faktiske fysiske flyten ved bruk av flytbasert markedskobling enn ved den nåværende metoden ved bruk av ATC [41].

For å takle usikkerhet tilknyttet endring i sammensetning av kraftproduksjon jobber SINTEF Energi med å utvikle en kort-tids fundamental flermarkedsmodell for å kunne prissette alle produkter i kraftmarkedet, for å bedre investeringsbeslutninger for nettoppgraderinger og kraftverk.

Masteroppgaven er utført med mål om å bidra til videre utvikling av modellen, PriMod, ved å implementere flytbasert markedskobling, for å øke modellens nøyaktighet i et fremtidig kraftsystem. Videre analyserer masteroppgaven hvordan implementasjonen påvirker modellen gjennom simuleringer, både i form av kraftflyt og endringer i prisene.

Resultatene fra simuleringene er lovende i en økonomisk sammenheng. Simuleringene viser at flytbasert markedskobling gir konvergerende priser i høyere grad enn den originale modellen. Videre argumenteres det for at den flytbaserte metodikken gir mindre opphopning av kraft i linjene, med mindre begrensende flaskehalser, ettersom kraften står friere til å følge den fysiske flyten. Utover de positive resultatene blir det diskutert "ikke-intuitiv" flyt av kraft. Dette konseptet må bli undersøkt av kraftprodusentene, ettersom kraften kan flyte mot en lavere priset sone. Til slutt blir forslag til forbedringer og utvidelser ved modellen presentert, både for økt nøyaktighet, og for å modelere andre interessante aspekter ved markedet.

Preface

This master's thesis was written the spring semester of 2019 and concludes my degree as Master of Science in Energy and Environmental Engineering at the Norwegian University of Science and Technology, NTNU, with the Department of Electric Power Engineering. Senior Research Scientist at SINTEF and Associate Professor at NTNU, Arild Helseth supervised the master's thesis, with the co-supervisors Associate Professor Hossein Farahmand, and Ph.D Candidate Christian Øyn Naversen.

I am grateful for the guidance I have received from my supervisors during the master's thesis, and the specialization project, prior to the master's thesis. You have been motivating, and provided me with the necessary tools to continue within the field of electrical power markets.

Further, I would like to thank the researchers at SINTEF Energy Research in the PRIBAS project for giving me access to the model, PriMod, and to provide insight into the work of scientists.

Lastly, I would like to thank the members of EMESP, and my co-students at the Department of Electric Power Engineering for the interesting discussions and colloquiums concerning topics related to my master's thesis.

Trondheim, June 13, 2019
Torbjørn Røed Meberg

Table of Contents

List of Tables

List of Figures

Abbreviations

AC	=	Alternating Current
ATC	=	Available Transfer Capacity
Core CCR	=	Core Capacity Calculation Region
CWE	=	Central Western Europe
DC	=	Direct Current
DS	=	Deferred Settlement
EFI	=	Norwegian Research Institute of Energy Supply, now SINTEF
EFTA	=	European Free Trade Association
EMPS	=	EFI's Multi-area Power-market Simulator (Samkjøringsmodellen)
EPAD	=	Electricity Price Area Differentials
FanSi	=	Scenario Fan Simulator
FBMC	=	Flow-Based Market Coupling
GSK	=	Genereation Shift Key
HVDC	=	High-Voltage Direct Current
NTC	=	Net Transfer Capacity
OPF	=	Optimal Power Flow
PPA	=	Power Purchase Agreement
PRIBAS	=	Pricing Balancing Services in the Future Nordic Power Market
PTDF	=	Power Transfer Distribution Factors
RES	=	Renewable Energy Sources
RHS	=	Right Hand Side
TRM	=	Transmission Reliability Margin
TSO	=	Transmission System Operator

Chapter 1

Introduction

1.1 Background

The European Union has recognized the challenges that come with climate change, and have set ambitious targets in order to reduce the emissions of greenhouse gases, carbon dioxide, CO_2, and Methane, CH_4. The aim towards 2050 is a reduction by 80-95% in emissions compared to 1990, through financing of renewable energy sources, energy savings and improvement of legislation [11]. Although Norway is not a member-state of the European Union, it is committed through EFTA, and is following the EU legislation on energy [7] and climate action [8].

The transition in the generation and use of power is causing new patterns of power flow and production. Upgrading of existing buildings, and regulations will lead to more energy-efficient buildings. This causes a decrease in the energy consumption in households and the service industry.

Electrification of current industry and transportation, in addition to new energy intensive industries, will increase the total load in the Norwegian

power system [37]. There is an ongoing discussion regarding to what extent the production needs to be upgraded, but an increase is certainly necessary in either scenario.

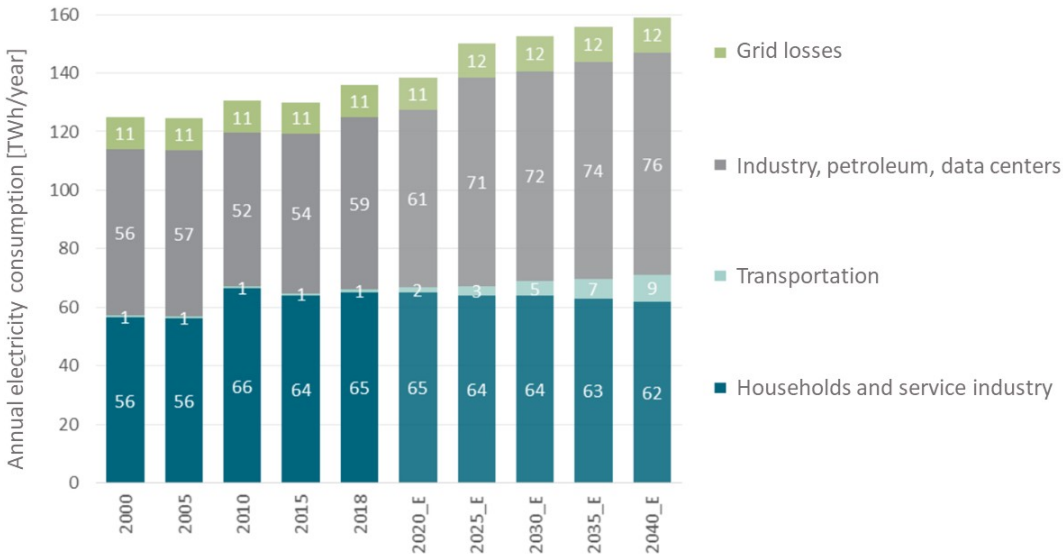

Figure 1.1: Electricity consumption mainland Norway expected towards 2040 [37]

The higher level of RES penetration in the power system and increase in load must of course be covered through an increased flow of power. The intermittent RES units will be uncontrollable in terms of time of production, thus requiring more flexibility and capacity in the transmission lines. Investment in new, or upgrading existing lines is capital intensive. The responsible party for the transmission network, the transmission system operator (TSO) is naturally interested in activities that may lower the cost of investment. The current five year investment plan to the Norwegian TSO, Statnett, is projecting 40-50 billion NOK spent between 2017 and 2021 in activities for upgrading the power grid [40].

1.2 Motivation

Lately, there has been a transition in how the European power markets are coupled. The concept of flow-based market coupling has gained support among the TSOs, as a more efficient method, than the conventional ATC market coupling mechanism. The benefits from the FBMC have made it the proposed method of achieving an interconnected European power system.

In the European power markets, the TSOs are working on increasing the total social surplus through a more efficient resource allocation, in terms of electricity. This could be achieved through the day-ahead markets where a converging price between zones could prove beneficial. In CWE (Central Western Europe), a change from the conventional capacities set by the ATC, to flow-based constraints, an increase in socio-economic surplus to 90% of the system optimum is expected. The optimum is as regarded the grid without limits on the capacities in the transmission lines [36].

Flow-based market coupling is currently in the planning phase in the Norwegian system, where the plan of the TSO is to start using it in 2021 [22] [41]. FBMC is already in use in the CWE, and will go live in Core CCR (Core capacity calculation region) in Q4 2020 [10].

1.3 Problem Formulation

Power systems are complicated structures, and to be able to understand them, advanced models have been created. PRIBAS is an ongoing project at SINTEF Energy Research, where the goal is to create a model concept that is able to calculate marginal costs for all physical products on a fine

time scale [18]. The model under development is called PriMod, and is a deterministic short-term model for hydro-thermal scheduling. In contrast to conventional calculations methods, the scope of the optimization is of a multi-market model, able to maintain the detail that producers require to operate the plants.

The scope of this master's thesis is to continue the development of SINTEF's model PriMod. Currently, the model is using a transport model for transferring power between the areas. The work will focus on how to incorporate flow-based market coupling to the model, and how the concept affects the behaviour of the simulated system compared to the present transmission modelling.

The work-flow will be to first get familiar with the model and the programming language. The data-sets will be examined in order to correctly implement flow-based market coupling. Further, the student will investigate previous work done on the field of research.

After completion of the initial work, FBMC will be implemented in the model, prior to an analysis of the results of the simulation. The analysis will try to discover changes in flow of power, and the associated effects in the pricing structure between the original model, and the modified version with FBMC.

Chapter 2

Theoretical Background

This chapter intends to supply the reader with the needed prerequisites of the theoretical background of this project. First, a brief presentation of important papers to this thesis will be provided. Further, an overview of the Nordic power market is presented as this forms the foundation of the price and bidding structure, that the simulated system is imitating. Last, the theory behind flow-based market coupling is presented. Physical relations within the field of power systems, from AC-flow to FBMC, are presented.

2.1 Related Research Projects

In this section, an overview of selected projects and papers related to PriMod and hydro-thermal scheduling, in addition to implementation of flow-based market coupling, will be presented.

Multi-Market Price Forecasting in Hydro-Thermal Power Systems [19] describes how strategic long-term models can be coupled with shorter-term operational models. This article details the short-term model PriMod and its coupling to the strategic model FanSi [20]. In addition to the coupling

between strategic and operational model, the mathematical formulations are presented together with a case study regarding weekly operation. The paper discusses the progress of the project and further work, where the intention is to extend the model to improve the imitation of the market and technical details.

A hydro-thermal market model for simulation of area prices including detailed network analyses [21] presents a market model for medium- and long-term scheduling, with a method of implementing flow-based market coupling. Market coupling is introduced to the stochastic EMPS model to handle bottlenecks in the grid. The paper provides the mathematical formulations of the implementation and network analyses on a four-part test system. The extended model was tested for a larger system, and the results were promising in terms of power flow, prices and generated power.

Flow-based market coupling and bidding zone delimitation: Key ingredients for an efficient capacity allocation in a zonal system [36] discusses allocation mechanisms, and how flow-based market coupling can provide the market with true competition for the capacity. The paper argues that a FBMC allocation method provides all exchanges to compete on equal terms, subject to the scarce capacity.

Impact of Generation Shift Key determination on flow based market coupling [4] provides areas of improvement for the FBMC-method trough generation shift keys. The paper presents different methods of calculating GSKs, and how the different methods hold different results for level of congestion, prices and ultimately social welfare.

2.2 The Nordic Power Market

After the deregulation of the Norwegian power market in 1991, the transmission system operator, Statnett, was given permission to operate an independent market in 1993, Statnett Market AS. The exchange was an open market, to facilitate competition between the actors, and thus increasing the efficiency in distribution of power. In 1996 the Norwegian and Swedish interconnected market was established, and the power exchange was renamed NordPool ASA. After this, more countries were included in the market over time, and is now comprised of the Nordic, Baltic and UK bidding zones. The volume of traded power has increased from 18.4 TWh in 1993 to 524 TWh in 2018 [27].

The power exchange will facilitate the flow of power from production to consumption. NordPool is a marketplace that enables the producers to sell, and suppliers to procure power for their customers in a bidding auction. The produced power is sold from the producers to the retailer for the consumption of the end-user, while delivered by the transmission and distribution system operators.

There are three main actors to control the markets; where the financial market is traded at NASDAQ OMX, the delivered power on NordPool, and the balancing market is operated by the TSO, Statnett. The balancing services are divided based on their response time, and consequently on the time of activation. They are denominated primary, secondary and tertiary reserves, and could be both up and down regulation [16]. The participators in the balancing market will be paid a premium to be on stand-by, to react if the TSO requires the service [42].

The structure of the power market is presented in figure 2.1, where the time of agreement stands in relation with the horizon of delivered power. The market consists of physical and financial products, where the latter is a market to adjust risk, or price hedging, with long-term contracts that could span for several years. The following section is based on the report published by the Norwegian Ministry of Petroleum and Energy [16].

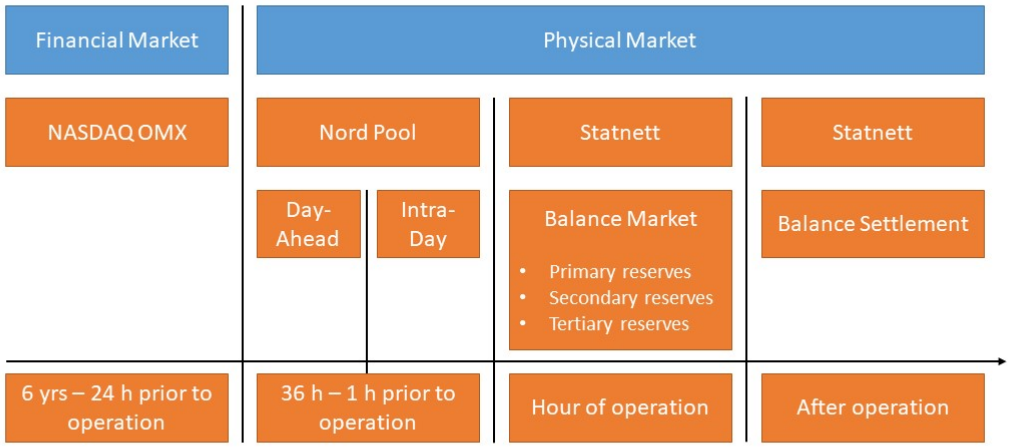

Figure 2.1: Market structure, with time relative to hour of operation on the axis [16]

2.2.1 Financial Market

Some actors in the power market may require predictability in the price of electricity. They can therefore choose to participate in the financial market to hedge against rising or falling prices for power. This could be used in speculative trading, or for large consumers of power, e.g. energy-intensive industries, to avoid peaking prices. Producers, consumers, or independent

actors that are engaging in speculative trading, may conduct a trade at NASDAQ OMX, when an agreement between two entities is available. The security of expected revenues and price of risk are the main drivers in the volatile financial markets.

The traded contracts in the financial market are usually long-term contracts, that could span from weeks to up to six years [16]. This is done in order to achieve long-term predictability to secure an acceptable price for a high-intensive consumer, or for a producer that needs to have a price over a certain limit. There is no delivered power from the financial trading, only payments from the opposing bet in accordance to the previously agreed contract. The financial market does not consider congestion management, or other local, physical limitations in the grid. The considered price for the contract is therefore the system price provided by NordPool.

NASDAQ OMX provides tradable power derivates at the exchange. These are EPADs, futures, DS futures and options. The difference between options and futures is the ability to choose whether to exercise the agreement of the fixed future price. However, this contract will come at the cost of premiums prior to the point of execution. The premiums are a way to measure and to put a price of the risk associated with the contract, and are determined on different factors such as season, current spot price and level of inflow [17]. Base and peak load are the listed contracts, that could be traded either with futures or DS futures. The difference between normal futures and DS futures, is the pay-off structure. Deferred settlement provides the actors to aggregate the losses or gains, and the mark-to-market will be realized upon delivery, in contrast to the daily payments from futures [25].

Electricity price area differentials, or EPAD is an instrument that considers the difference in prices between areas. This allows members to hedge against risk of congestion in the grid, thus increasing or decreasing the price in the area [25]. The concept of congestion and prices is further explained in section 2.2.2.

A power purchase agreement, PPA, is more of an incentive to give the producer a reliability to invest in more power, and is not traded at NASDAQ OMX, as it is an bilateral agreement [43]. A buyer commits to buy a predetermined amount of energy to a given price from a producer. The PPAs will reduce the price of risk concerning profitability of the plants, thus increasing the net present value of a power plant [26].

2.2.2 Day-Ahead Market

The physical market is where the actual power is traded, and is mainly done on the day-ahead market. NordPool is the operator of the day-ahead market, and acts as a guarantor of delivery to the market. The power for the next day is traded on an hourly basis, where the market closes at 12:00 Central European time, for the next day.

The price in the market depends on the supply and demand, that together form the spot price for the market in the relevant hour of the next day. This economic mechanism will create an initial balance between produced and consumed power, where the price is the intersection between supply and demand in figure 2.2 [31].

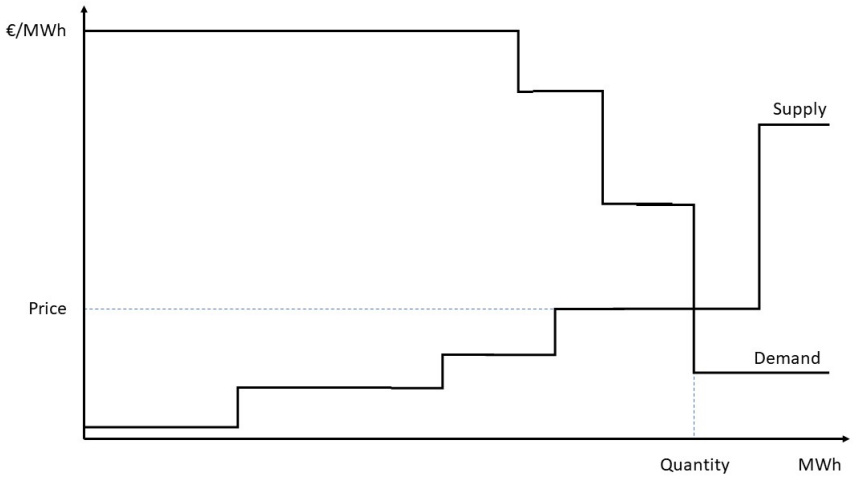

Figure 2.2: Supply and demand, formation of spot price [16]

The day-ahead market for the Nordics consists of fifteen zones, five in Norway, four in Sweden, two in Denmark, and one for each of Finland, Estonia, Latvia and Lithuania. Inside these zones, the price is equal, and the system is thus zonal priced. The limited transfer capacity between the different zones, is forcing price differences between zones, as some areas have a power surplus, while others may have a higher demand [29]. The TSO is setting constraints to the grid based on assumptions of the capacity of transfer [16].

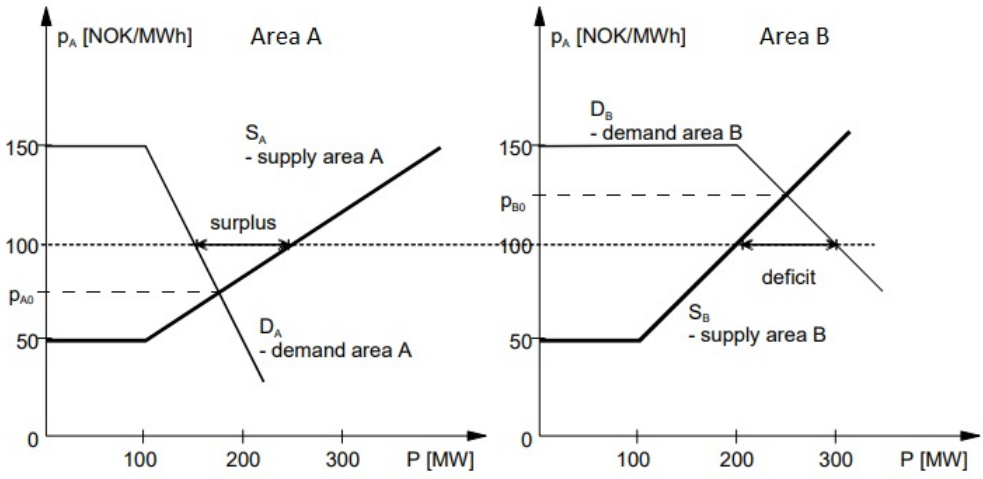

Figure 2.3: Price adjustment for trading between zones [12]

The structure of the market will generate different local price structures with supply and demand, where the available transferred power will affect the neighbouring area based on the price differences. Figure 2.3 is introduced to illustrate the concept, where area B has a greater demand than A, and other costs such as congestion rate and other tariffs are neglected. Initially area A has a price of 75 NOK/MWh, and B has 125 NOK/MWh, if no power is transferred. If the two areas are interconnected with sufficient capacity, area A is able to sell power in Area B, thus forming one single price structure and increasing total social welfare, with equal pricing of 100 NOK/MWh in the two areas [12].

2.2.3 Intra-Day Market

As the power system is dependent on the weather, on both the production and demand side, the initial balance may be altered to the next day. Wind, sunlight, inflow of water, and temperature all contribute to the use and production of power and are subject to uncertainty. When a correction in the

power balance is required, the actors in the marketplace may use the intra-day market, to either sell or procure power for the relevant hour of trade.

For actors in the Nordic power market, the intra-day exchange Cross-Border Intraday Market (XBID) provides the opportunity to trade power until 60 minutes prior to the operating hour [30]. NordPool operates a cross-border intra-day trading with 13 countries, including the Nordics, Balticum, the UK, France, Germany, Austria, Belgium and the Netherlands. XBID went go-live the 12/06/2018 [28].

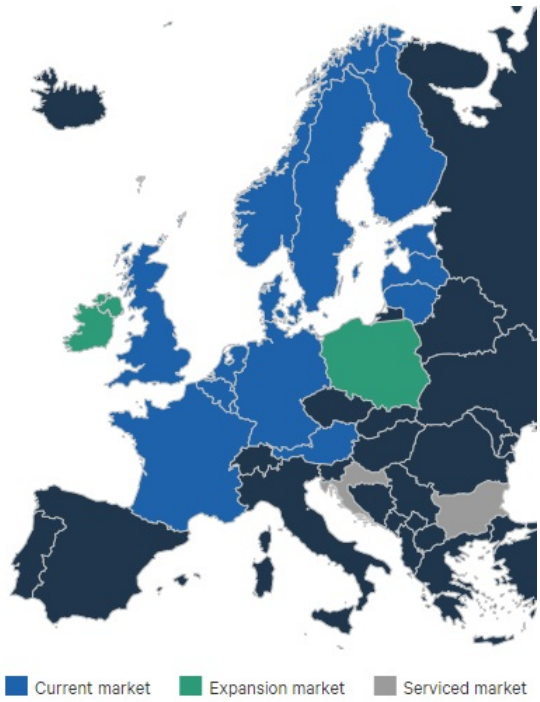

Figure 2.4: XBID market [30]

The cross-border connections are important tools for increasing the liquidity of the market, and the ability to balance the market [33].

2.3 AC Power Flow

The power flowing in the grid, is an alternating current, AC. To be able to model the network, a thorough understanding of the fundamental AC power flow is needed. Power flow equations form the basis of theory of electrical engineering within transmission systems, and could therefore be found in a series of literature. This section is based on [45].

The power comprise of a real, P, and a reactive part, Q, to form the complex power, S.

$$S = P + jQ = \mathbf{V} \cdot \mathbf{I}^* \tag{2.1}$$

The asterisk denotes the conjugate of the current. In a network of nodes, the current could be represented as a vector dependent on the admittance matrix and the voltage vector. The admittance matrix or Y-bus is constructed to model the admittance of the grid, where the single element represents the line between the nodes from the row and column. Further, the diagonal elements will represent the total admittance of connected lines to the node [45].

$$\begin{bmatrix} I_1 \\ \vdots \\ I_n \end{bmatrix} = \begin{bmatrix} Y_{1,1} & \cdots & Y_{1,n} \\ \vdots & \ddots & \vdots \\ Y_{n,1} & \cdots & Y_{n,n} \end{bmatrix} \cdot \begin{bmatrix} V_1 \\ \vdots \\ V_n \end{bmatrix} \tag{2.2}$$

For a node *i* in the network the current I_i will be the following.

$$I_i = Y_{i,1} \cdot V_1 + \cdots + Y_{i,i} \cdot V_i + \cdots + Y_{i,n} \cdot V_n = \sum_{j=1}^{n} Y_{i,j} \cdot V_j \tag{2.3}$$

Substituting 2.3 to 2.1 yields

$$S_i = V_i \cdot \left(\sum_{j=1}^{n} Y_{i,j} \cdot V_j \right)^* = V_i \cdot \sum_{j=1}^{n} Y_{i,j}^* \cdot V_j^* \tag{2.4}$$

When Eulers identity is applied $e^{j\delta} = cos(\delta) + jsin(\delta)$ and that $Y_{i,j} \equiv G_{i,j} + jB_{i,j}$ the following is obtained from 2.4.

$$\begin{aligned} S_i =& |V_i| e^{j\delta_i} \sum_{j=1}^{n} |V_j| (e^{j\delta_j})^* (G_{i,j} + jB_{i,j})^* \\ =& \sum_{j=1}^{n} |V_i||V_j| e^{j\delta_i - j\delta_j} (G_{i,j} - jB_{i,j}) \\ =& \sum_{j=1}^{n} |V_i||V_j| \left(cos(\delta) + jsin(\delta)\right) (G_{i,j} - jB_{i,j}) \end{aligned} \tag{2.5}$$

Separating the real and imaginary values to obtain the real and reactive power, as equation 2.1.

$$P_i = \sum_{j=1}^{n} |V_i||V_j| \left(G_{i,j} \cdot cos(\delta_{i,j}) + B_{i,j} \cdot sin(\delta_{i,j})\right) \tag{2.6}$$

$$Q_i = \sum_{j=1}^{n} |V_i||V_j| \left(G_{i,j} \cdot sin(\delta_{i,j}) - B_{i,j} \cdot cos(\delta_{i,j})\right) \tag{2.7}$$

The equations 2.6 and 2.7 are the two power flow equations for respectively real and reactive power for a bus i [45].

2.4 DC Approximation

In a large power system, the AC power flow computations become complex and time-consuming. One can also run into convergence problems due

to the non-convexity of the AC power flow equations. Thus, methods for power flow calculations based on DC approximation have been developed, allowing for a reduction in computational time and avoid use of unreliable or not available data. The DC-approximation could be found derived in textbooks for electrical engineering, this section is based on [44].

Several assumptions are performed in order to compute a DC power flow. The voltages are assumed to be close to its nominal value, and therefore $V_i = 1.0\ [p.u.]$. Further, the reactances are higher than the resistances, thus assuming that $x_i >> r_i$, making $z_i = jx_i$. From the Y-matrix, all diagonal values will have the angle $-\pi/2$, and $+\pi/2$ for the off-diagonal values. Further, the angle $\Delta\delta$ can be approximated as $sin(\delta) = \delta$ and $cos(\delta) = 1.0$ as $\Delta\delta$ is considered small, $\pm$ 0.05.

Applying the term $G_{i,j} + jB_{i,j} = Y_{i,j}\angle\theta_{i,j}$ and $\delta_{i,j} = \delta_i - \delta_j$ to the AC power equations 2.6 and 2.7, the power equations are written as the following [6].

$$P_i = \sum_{j=1}^{n} |V_i||V_j|Y_{i,j} \cdot cos\left(\delta_i - \delta_j - \theta_{i,j}\right) \tag{2.8}$$

$$Q_i = \sum_{j=1}^{n} |V_i||V_j|Y_{i,j} \cdot sin\left(\delta_i - \delta_j - \theta_{i,j}\right) \tag{2.9}$$

Further, considering that $cos(x - \pi/2) = sin(x)$ and using the aforementioned approximations, the DC power flow will be the following, as the reactive power is eliminated.

$$P_i = \sum_{j=1}^{n} Y_{i,j} \cdot (\delta_i - \delta_j) \tag{2.10}$$

The DC approximation can then be written as a matrix. The sum of the

power flows to or from node i is dependent on the assigned direction of the flow [44].

$$\begin{bmatrix} P_1 \\ \vdots \\ P_n \end{bmatrix} = \begin{bmatrix} Y_{11} & \cdots & Y_{1n} \\ \vdots & \ddots & \vdots \\ Y_{n1} & \cdots & Y_{nn} \end{bmatrix} \cdot \begin{bmatrix} \delta_1 \\ \vdots \\ \delta_n \end{bmatrix} \tag{2.11}$$

2.5 Flow-Based Market Coupling

The flow based market coupling is based on the concept of power transfer distribution factor, $a^n_{i,j}$, that is used to describe the change in the flow of power in respect of an injection in the grid.

The PTDF consists of elements from both the Y_{bus}, or Y-matrix, and the Z_{bus}, which is the inverted $Y_{bus}$where the slack-bus i has added $+1$ prior to the inversion [35].

$$Y_{bus} = \begin{bmatrix} \sum_{j=1}^{n} B_{1,j} & \cdots & -B_{1,n} \\ \vdots & \ddots & \vdots \\ -B_{n,1} & \cdots & \sum_{j=1}^{n} B_{n,j} \end{bmatrix} \tag{2.12}$$

$$Z_{bus} = \begin{bmatrix} \sum_{j=1}^{n} B_{1,j} + 1 & \cdots & -B_{1,n} \\ \vdots & \ddots & \vdots \\ -B_{n,1} & \cdots & \sum_{j=1}^{n} B_{n,j} \end{bmatrix}^{-1} \tag{2.13}$$

For a line from node i to j with an injection from node n, the PTDF can be calculated as the following. Rearranging equation 2.11 to $\Delta\delta = Z_{bus} \cdot \Delta P$ the following can be obtained.

$$\Delta\delta_i = Z_{bus,i,n} \cdot \Delta P_n \tag{2.14}$$

$$\Delta\delta_j = Z_{bus,j,n} \cdot \Delta P_n \tag{2.15}$$

$$\Delta P_{i,j} = Y_{i,j} \cdot (\Delta\delta_i - \Delta\delta_j) \tag{2.16}$$

Substituting equation 2.14 and 2.15 in 2.16, and assuming that ΔP_n is 1.0, the PTDF is obtained.

$$a_{i,j}^n = Y_{i,j} \cdot (Z_{bus,i,n} - Z_{bus,j,n}) \tag{2.17}$$

Equation 2.17 can be organized in a matrix where the nodes of injection are the columns, and the lines in the network are sorted in the rows.

$$a_{i,j}^n = \begin{bmatrix} a_{1,2}^1 & \cdots & a_{1,2}^n \\ \vdots & \ddots & \vdots \\ a_{i,j}^1 & \cdots & a_{i,j}^n \end{bmatrix} \tag{2.18}$$

The flow of a line $f_{i,j}$ can be calculated in equation 2.19 with the sum of the PTDF value of the line and the net power at the buses. Further, the flow of the line needs to be within the capacity limits of the line, B, as in equation 2.20.

$$f_{i,j} = \sum_{n \in N} a_{i,j}^n \cdot P_n \tag{2.19}$$

$$-B \leq \sum_{n \in N} a_{i,j}^n \cdot P_n \leq B \tag{2.20}$$

The net position of power in two corresponding zones will be constrained by how much power that the transmission lines are able to transfer in or out of the zone. The domain of the NTC will be constrained by the sum of capacity in the lines connected to the zone in both directions, with a transmission reliability margin (TRM) taken into account. The ATC will, similarly to NTC, be based on the capacity and TRM, but will also consider the planned physical flow for the following 24 hours, decided by the TSO, thus forming a smaller domain than the NTC, as illustrated in figure 2.5 [9].

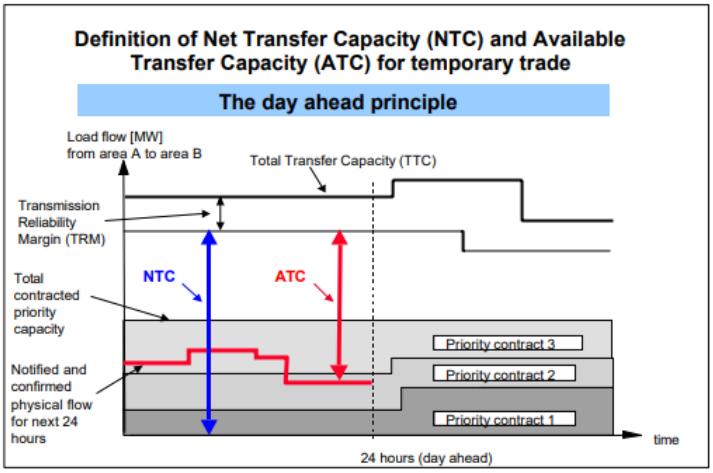

Figure 2.5: Day-ahead principle using NTC and ATC in the Nordel-area [9]

The flow-based market coupling will be constrained by the PTDF-matrix, thus constructing a different domain of opportunity. In figure 2.7 the domain of the flow-based, ATC, and NTC scenarios are illustrated.

An example is provided to illustrate how the domain of the net injected power with flow-based market coupling is constructed. Consider that a system of three areas in figure 2.6 has the following PTDF-values in table 2.1.

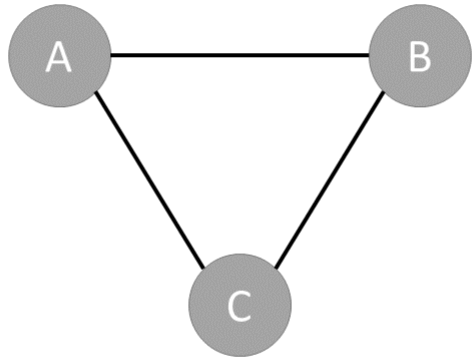

Figure 2.6: Connected 3-area system [35]

Line	Maximum flow	Influence from A	Influence from B	Influence from C
A - B	1000 MW	0.33	-0.33	0
B - C	1000 MW	0.33	0.67	0
A - C	1000 MW	0.67	0.33	0

Table 2.1: PTDF-values 3-area system [35]

If the ATC is available to operate at 75% of the NTC, each line can operate at the maximum 750 MW, creating the red ATC domain in figure 2.7. The areas are exporting power when the value is positive on their axis, and similarly, importing if it is negative. The PTDF-values from table 2.1, coupled with the limits of the lines, create the yellow domain in figure 2.7. The constraints for the flow-based domain are labeled with the line and direction of flow. To illustrate how the constraints are computed, A - C is considered. On the axis of A, the cable's maximum capacity divided by the contribution form area A, $\frac{1000MW}{0.67} = 1500MW$. Similarly for area B, where the

contribution can be read from table 2.1, $\frac{1000MW}{0.33} = 3000MW$. This creates the two necessary points to plot the constraint, $(0, 1500), (3000, 0)$.

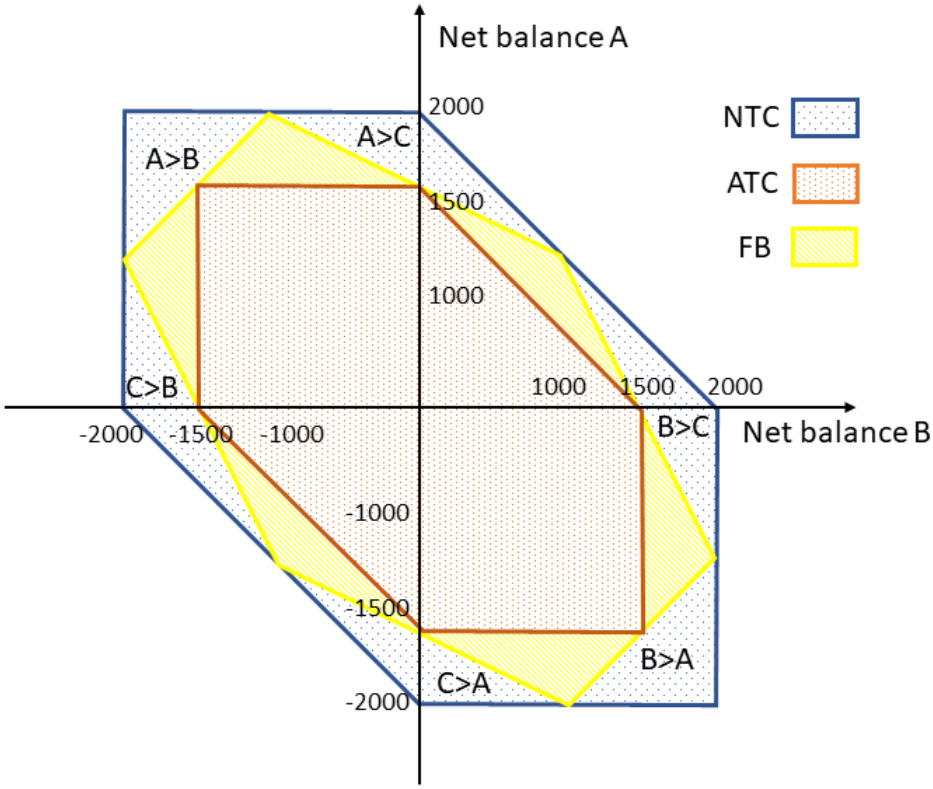

Figure 2.7: NTC, ATC and Flow-based domain [MW] [35]

From figure 2.7, the observation is that the domain constructed by the flow-based market coupling is greater than the domain of the conventional ATC, while not violating the constraints of the NTC. The constructed domain is the possible net injections of power for two areas.

The change from predetermined flow of power in the ATC, to the flow-based solution, where the flow is determined after clearing of the market based on the PTDF-restrictions in the clearing, leaves more room for the domain of the solution [39].

2.6 Generation Shift Keys

The PTDF equations are on a nodal format, and as the Nordic power market is organized in zones, the PTDFs need to be transferred to zonal equations. This is done with the generation shift keys, GSK, which level the different nodal PTDFs accordingly in the zonal PTDF [34].

$$a_{i,j}^{area} = \sum_{n \in N} GSK^n \cdot a_{i,j}^n \tag{2.21}$$

The concept of GSKs provides the ability to aggregate the nodal equations to zonal equations. However, there is not a determined standard convention on how to apply a strategy of calculating the GSKs, due to its dependence on the technology of production and demand side in the system. The chosen strategy has to consider type of generation and geographical or topological distribution of the grid. The strategy could be based on numbers of flexible units, numbers of generators, or net power, either varying over time or an average of previous measurements [4].

Another solution is applying a flat strategy. This strategy will be weighing the nodes within a zone equally, as the GSK for an area will be equation 2.22, where $\mathcal{N}$ is the total number of nodes in the studied area.

$$GSK^n = \frac{1}{\mathcal{N}} \tag{2.22}$$

The flat strategy is the first strategy that Statnett and the other Nordic TSOs are applying for the markets with the ongoing introduction of flow-based market coupling in the power grid. However, other strategies will be assessed, and may be implemented at a later stage [32]. There are running simulations with flow-based market coupling in parallel to the daily operation until the introduction of flow-based market coupling in late 2021 [22].

The impact of the GSK in the power system is big, where inaccuracies may lead to errors in the planning and operation of the grid, and thus need to be assessed properly before implementation.

Chapter 3

Method

The following chapter will present the method of implementation of flow-based market coupling in the model PriMod. First, an introduction to hydro scheduling is presented in order to correctly describe the model, with its scope, and scheduling horizon. Further, the model will be presented as an optimization problem, with a description of the constraints, prior to an explanation of the used data-set. Last, the implementation of the transmission grid with the PTDF-matrix will be presented.

3.1 Hydro Scheduling

The Norwegian energy production system consists mainly of hydro power, with a dominant share of the market as illustrated in figure 3.1. With a considerable opportunity to exchange power between countries through cross border connections, the Nordic power system is considered as a hydro-thermal system.

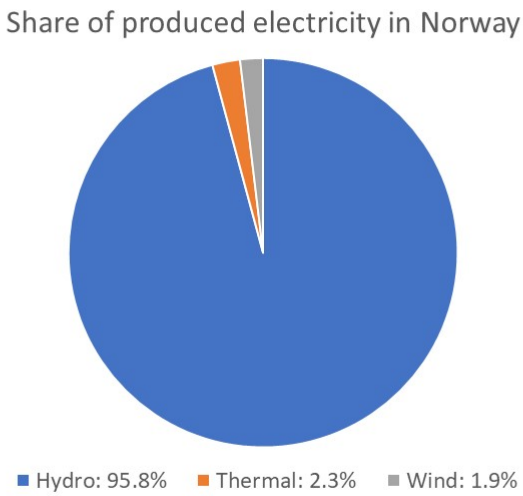

Figure 3.1: Norwegian composition of generation in 2017 [38]

The fuel for the hydro plants will come as inflow, either regulated or unregulated. The inflow of water may originate from upper reservoirs, rivers, rain or melted snow. The operators of the Norwegian power plants will therefore have a zero cost associated with acquiring the needed resources for the production. However, the inflow of water is not stable due to uncertainty, and opportunity for future profits will be dependent of the planning of dispatching the hydro.

To optimize the production of stored water in the reservoirs, there are three scheduling horizons that need to be considered and coupled before the dispatch of the stored water; long-term, seasonal-term, and short-term. The scheduling will be done in the order of the time horizon from the long-

to the short-term scheduling, where the detail of the results will increase with shorter time frame. Normally, the results from the long- and seasonal scheduling are updated each week, while the short-term scheduling needs to be performed at least every day [24].

To balance future and present profits, the concept of water values are introduced in hydro scheduling. The water values put a price on the otherwise free resource, where the cost of not being able to produce the dispatched hydro in the future affects the profits in the current scope of optimization. The values are characterized as cuts constraining the expected future revenue [5]. There are several advanced algorithms to compute the water values, and correct evaluation of the hydro will provide a higher profit for the decision maker for the plant [13].

3.1.1 Long-term scheduling

The long-term scheduling is done in order to find the optimal use of a plant with its reservoir for a long time frame, typically between one and five years. Inflow may vary annually, and with fluctuating prices, the analysis provides a foundation of data to make decisions on the long-term. The meteorological forecasts for several years in advance are not precise enough to make accurate decisions, thus forcing the scheduling to use statistical data and probability in order to get its results. The models are therefore considered to be stochastic. The most widely used model for the Nordics is the EMPS model [5].

3.1.2 Seasonal Scheduling

The seasonal scheduling provides a coupling between the long-term and short-term models. The long-term model has aggregated values, and as the

short-term optimization requires more detailed information, such as reservoir limits, e.g. the seasonal model is able to provide the data.

There is an overlap in time horizon between the long-term and seasonal scheduling. However, the planning horizon of the seasonal scheduling to actual production is dependent on the level of regulation in the system, where a higher degree requires a horizon further into the future. The seasonal scheduling could either be done with stochastic models, or simulations using a multiple scenarios [5].

3.1.3 Short-term optimization

The short-term scheduling uses deterministic models, due to the short timeframe of optimization. The short horizon coupled with a deterministic model provides the opportunity for a higher degree of detail, as inflow and water values are considered known parameters, not variables. The level of detail needs to be of a quality that allows the results from the simulations to be used in the actual operation of the plant [5].

3.2 PriMod: a short-term fundamental market model

SINTEF Energy Research has developed a deterministic model to simulate short-term scheduling on a hydro-thermal system. This section will explain its structure and the differences from other models for scheduling.

3.2.1 Scheduling

The model used for this analysis, PriMod, also referred to as *the model* has characteristics from both the long- and short-term scheduling. PriMod solves a deterministic weekly hydro-thermal scheduling problem, provided with weekly cuts from the FanSi model. The FanSi model is a long-term dynamic stochastic simulation [20].

PriMod is modeled in the open source programming language Python, with the modelling language Pyomo for optimization [15] [14]. The solver used in this thesis is CPLEX provided by IBM.

As the size of the systems usually decreases with shorter horizon of the scheduling to increase accuracy, the long-term scheduling analyses the power system, whereas short-term modeling more often solves an optimization for a reservoir system.

PriMod stands out from other models by using the complexity of the size of the long-term model, while providing detailed prices as it is a short-term model. The reason for this is the framework that couple the the long- and short-term models [19]. The horizon of modeling for the model is one to two weeks, with a broad scope that accounts for the whole power system. The horizon of the optimization are as aforementioned, provided by the strategic long-term model, FanSi, in figure 3.2. The cuts are water values, or strategies on what the planning is optimizing for.

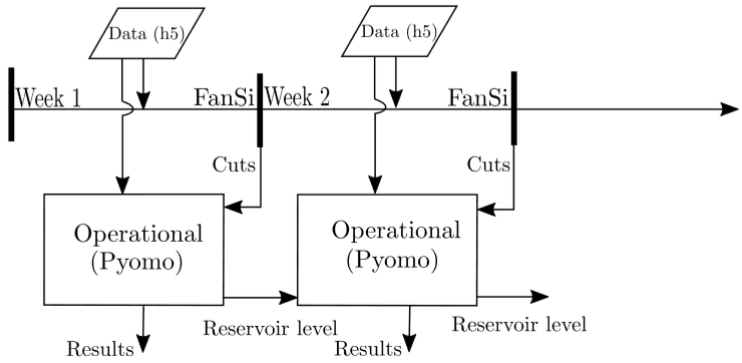

Figure 3.2: Flowchart of PriMod (Operational) with FanSi (Strategic) [19]

3.2.2 Optimization

It is necessary to declare the indexes, sets, parameters and variables in order to explain the optimization performed in PriMod [34]. The model is presented with the mathematical formulations prior to the implementation.

Indexes:

k	Timesteps
a	System area
c	Cuts
t	Week
r	Reservoir
i	From area
j	To area
n	Market step
p	Segment

Sets:

$\mathcal{A}$	Price areas
$\mathcal{T}$	Weeks
$\mathcal{K}_t$	Timesteps in week t
$\mathcal{C}_t$	Cuts in week t
$\mathcal{M}_a$	Market steps per area
$\mathcal{R}_a$	Reservoirs in area a
$\mathcal{R}_a^{reg}$	Regulated reservoir in set a
$\mathcal{R}_r^{pump}$	Pumping reservoir r
$\mathcal{S}_r^{PQ}$	Segments of piecewise linear PQ
$\mathcal{W}_a$	Wind parks in area a

Parameters:

$\mathcal{T}_{i,j}^{cap}$	Transmission capacity line i to j
$\mathcal{T}_{i,j}^{loss}$	Transmission loss from area i to j
$\mathcal{M}_{n,k}^{price}$	Market price market step i, step k
$\mathcal{M}_{n,k}^{Cap}$	Market capacity step i, step k
$\mathcal{L}_{a,k}$	Aggregated area loads step k
$\mathcal{W}_{a,k}$	Wind production step k
$\mathcal{R}_{r}^{max}$	Maximum reservoir capacity r
$\mathcal{R}_{r}^{min}$	Minimum reservoir r
$\mathcal{R}_{r}^{init}$	Start reservoir r
$\mathcal{R}_{r}^{max\ byp}$	Maximum bypass reservoir r
$\mathcal{R}_{r}^{min\ byp}$	Minimum bypass reservoir r
$\mathcal{R}_{r}^{max\ dis}$	Maximum discharge reservoir r
$\mathcal{R}_{r}^{min\ dis}$	Minimum discharge reservoir r
$\mathcal{Q}_{p}^{PQ}$	Discharge volume per PQ-curve segment p
$\eta_{r,p}^{PQ}$	Generation efficiency per PQ segment p
$\mathcal{H}_{r}^{h/h_0}$	Relative head at r, referred to initial reservoir
$\mathcal{Q}_{r}^{pump}$	Pump power form reservoir r
$\mathcal{I}_{r,k}^{reg}$	Regulated inflow reservoir r
$\mathcal{I}_{r,k}^{unreg}$	Unregulated inflow reservoir r
β_c	Cut RHS cut c
$\pi_{r,c}$	Cut coefficient reservoir r, cut c
$\mathcal{P}^{tank}$	Tank water cost
$\mathcal{P}^{spill}$	Spillage penalty
$\mathcal{P}^{byp}$	Bypass penalty

Variables:

$t_{i,j,k}$	Transmission from i to j in timestep k
$m_{n,k}$	Purchase or sale (+/-) in market step area, step k
$x_{r,k}$	Reservoir level reservoir r, step k
$q_{r,k}$	Release from reservoir r, step k
$q^{dis}_{r,p,k}$	Discharge from reservoir r, segment p, step k
$q^{spill}_{r,k}$	Spillage reservoir r, step k
$q^{byp}_{r,k}$	Bypass reservoir r, step k
$q^{pump}_{r,k}$	Pumping reservoir r, step k
$q^{tun}_{r,k}$	Tunneling between reservoirs r, step k
$q^{tank}_{r,k}$	Tanking reservoir r, step k
α	Future profit function
$p^{hydro}_{r,k}$	Production per module/reservoir r, step k

The optimization is performed as described in the following, where the goal is to optimize the objective function subject to its associated constraints. The problem is solved for all $a \in \mathcal{A}$, $t \in \mathcal{T}$, $k \in \mathcal{K}_t$ and $r \in \mathcal{R}_a$.

Objective function

The objective of power scheduling is to maximize the profit, thus leading the optimization to be a minimization of the production costs and avoiding misuse of stored water.

$$min\ \pi = \sum_{k \in \mathcal{K}_t} \sum_{n \in \mathcal{M}_a} \sum_{a \in \mathcal{A}} \Bigg(\mathcal{M}_{n,k}^{price} \cdot m_{n,k} + \sum_{r \in \mathcal{R}_a} \left(q_{r,k}^{byp} \cdot \mathcal{P}^{byp} + q_{r,k}^{spill} \cdot \mathcal{P}^{spill} + q_{r,k}^{tank} \cdot \mathcal{P}^{tank} \right) \Bigg) + \alpha \tag{3.1}$$

Subject to:

Reservoir balance

The changes in the reservoir is dependent on the inflow, thus the upstream reservoirs are of importance. $r \in \mathcal{R}_{a,\ ups}$ is the denomination for the upstream reservoirs.

$$\mathcal{I}_{r,k}^{reg} = x_{r,k} - x_{r,k-1} + q_{r,k} + q_{r,k}^{spill} + q_{r,k}^{pump} - q_{r,k=1}^{tank} - \sum_{r \in \mathcal{R}_{a,\ ups}} \left(q_{r,k}^{spill} + q_{r,k}^{pump} + q_{r,k}^{tun} - q_{r,k}^{tun} + \sum_{p \in \mathcal{S}_r^{PQ}} q_{r,p,k}^{dis} \right) \tag{3.2}$$

Release balance

The unregulated inflow is equal to the bypassed and sum of discharged water.

$$\mathcal{I}_{r,k}^{unreg} = q_{r,k}^{byp} - q_{r,k} + \sum_{p \in \mathcal{S}_r^{PQ}} q_{r,p,k}^{dis} \tag{3.3}$$

Hydro power balance

The produced hydro for an area must comply with the import and export to cover the aggregated load.

$$\mathcal{L}_{a,k} - \mathcal{W}_{a,k} = \sum_{r \in \mathcal{R}_a} \left(\sum_{p \in \mathcal{S}_r^{PQ}} \left(\eta_{r,p}^{PQ} \cdot q_{r,p,k}^{dis} \cdot \mathcal{H}_r^{h/h_0} \right) - \mathcal{Q}_r^{pump} \cdot q_{r,k}^{pump} \right) + \sum_{n \in \mathcal{M}_a} m_{n,k} - \sum_{j \in \mathcal{A}} \left(t_{i,j,k} - t_{j,i,k} \cdot (1 - \mathcal{T}_{j,i}^{loss}) \right) \tag{3.4}$$

Thermal power balance

The thermal areas are modelled similarly as the hydro areas but without the hydro generating units and reservoirs.

$$\mathcal{L}_{a,k} - \mathcal{W}_{a,k} = \sum_{n \in \mathcal{M}_a} m_{n,k} - \sum_{j \in \mathcal{A}} t_{i,j,k} - t_{j,i,k} \cdot (1 - \mathcal{T}_{j,i}^{loss}) \tag{3.5}$$

Cut constraint

The expected future cost of operation must be greater than the RHS cuts β_c.

$$\alpha + \sum_{a \in \mathcal{A}} \sum_{r \in \mathcal{R}_a} \sum_{c \in \mathcal{C}_t} \pi_{r,c} \cdot x_{r,k} \geq \sum_{c \in \mathcal{C}_t} \beta_c \tag{3.6}$$

Limits for reservoir, bypass, discharge & transfer lines

During the optimization, the decision variables need to be within their limits. These limits are defined by their corresponding parameters. In addition to the following limits, there are limits for all other variables.

$$\mathcal{R}_r^{min} \leq x_{r,k} \leq \mathcal{R}_r^{max} \tag{3.7}$$

$$\mathcal{R}_r^{min\ byp} \leq q_{r,k}^{byp} \leq \mathcal{R}_r^{max\ byp} \tag{3.8}$$

$$\mathcal{R}_r^{min\ dis} \leq \sum_{i \in \mathcal{S}_r^{PQ}} q_{r,p,k}^{dis} \leq \mathcal{R}_r^{max\ dis} \tag{3.9}$$

$$0 \leq t_{i,j,k} \leq \mathcal{T}_{i,j}^{cap} \tag{3.10}$$

Generation

The generation is calculated as a post process for the problem, when the solver has found the solution.

$$p_{r,k}^{hydro} = \sum_{p \in \mathcal{S}_r^{PQ}} \eta_{r,p}^{PQ} \cdot q_{r,p,k}^{dis} \cdot \mathcal{H}_r^{h/h_0} \tag{3.11}$$

3.2.3 Pricing

An important trait of linear optimization problems is the possibility to do a sensitivity analysis, that provides a shadow price. The dual value of a restriction could be seen as the marginal cost, which proves useful when calculating a cost of a product in a competitive market, where the marginal cost is the deciding factor [1].

PriMod is calculating the prices of power by finding the dual of the power balance equations in 3.4 and 3.5. This will reflect the cost of producing one more unit of power, thus finding the market price.

The calculation of market prices in PriMod varies from NordPool. In the main market for purchasing power, the day-ahead market, bids of supply and demand are provided by bulk in portfolios as explained in section 2.2.2. This differs from the pricing at NordPool as the prices are determined by the intersection by supply and demand, not the cost of producing an extra MWh of power.

3.3 Data-sets

The data-set for the model, PriMod, that is used in the simulations is referred to as *4del*. This is a simplified grid system that contains four price areas to represent a hydro-thermal power grid. The four zones of operation are Numedal, Otra, TEV (Trondheim Energiverk), and Term. The three first zones represent classical Norwegian areas of production of power, dominated by hydro. The latter, Term, is modeling a connection to main Europe where thermal generation is one of the main contributors to the power system.

	Number of Reservoirs	Max Reservoir	Max Production
Numedal	17	931.0 Mm^3	610.2 MW
Otra	21	1946.6 Mm^3	819.5 MW
TEV	12	1381.9 Mm^3	535.3 MW
Term	-	-	314.14 MW

As modeled in section 3.2, the zones include a high degree of detail in the production of power from hydro. The discharge, relative height of the reser-

voir to the plant, and the piecewise linear PQ-curves of the plants all contribute to an accurate description of the produced power at each segment. The reservoir system is well represented, with the topology and connections between the different reservoirs. The data-set includes the aforementioned cuts for each week, that describe the cost of lost future revenues of the stored hydro.

The three hydro areas have some thermal capacities, these are modeled together with load that are elastic to price changes. This could be industries that are dependant on producing with a price of electricity below a certain threshold. Due to the coupling between elastic load and thermal production, the thermal production could be negative in an area.

The remaining load in the system is considered a parameter, as it is not dependent on price. The assumption is justifiable, as the scope of the scheduling is one to two weeks, and the simulations is deterministic, i. e. the uncertainties are considered known. Electricity demand can be considered inelastic in the short-term as there are no available substitutes for the consumer in the planning period [2].

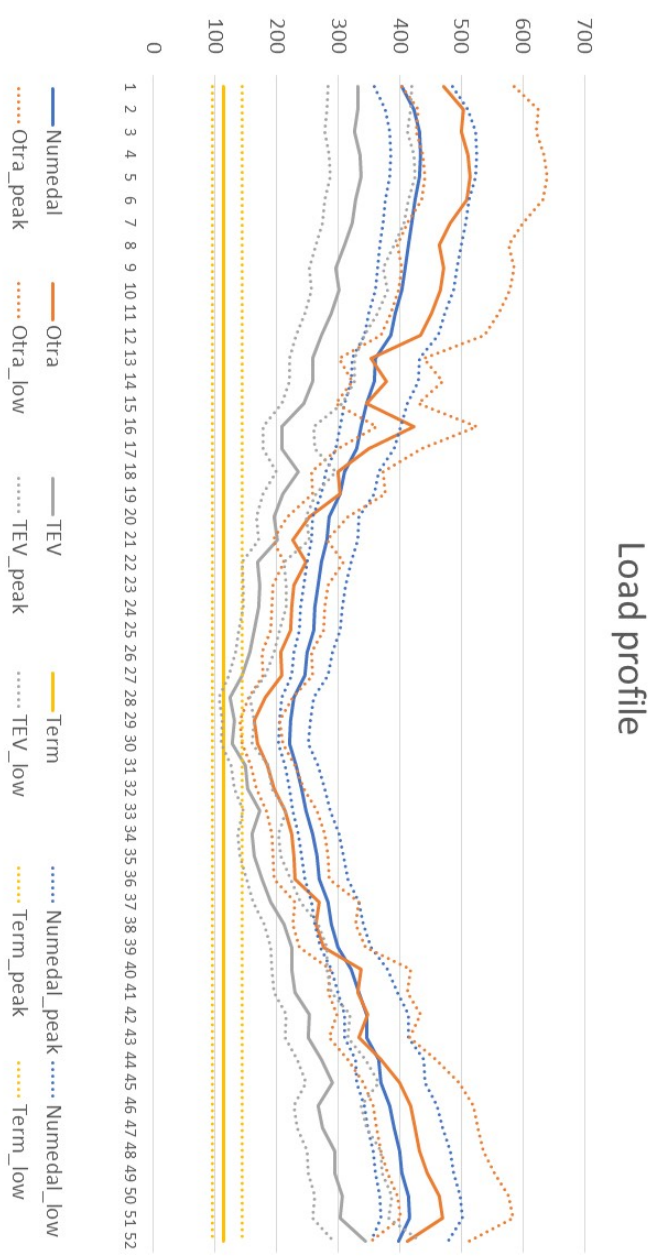

Figure 3.3: Weekly average load (without thermal), with peak and lowest base load for the four zones over the simulated year

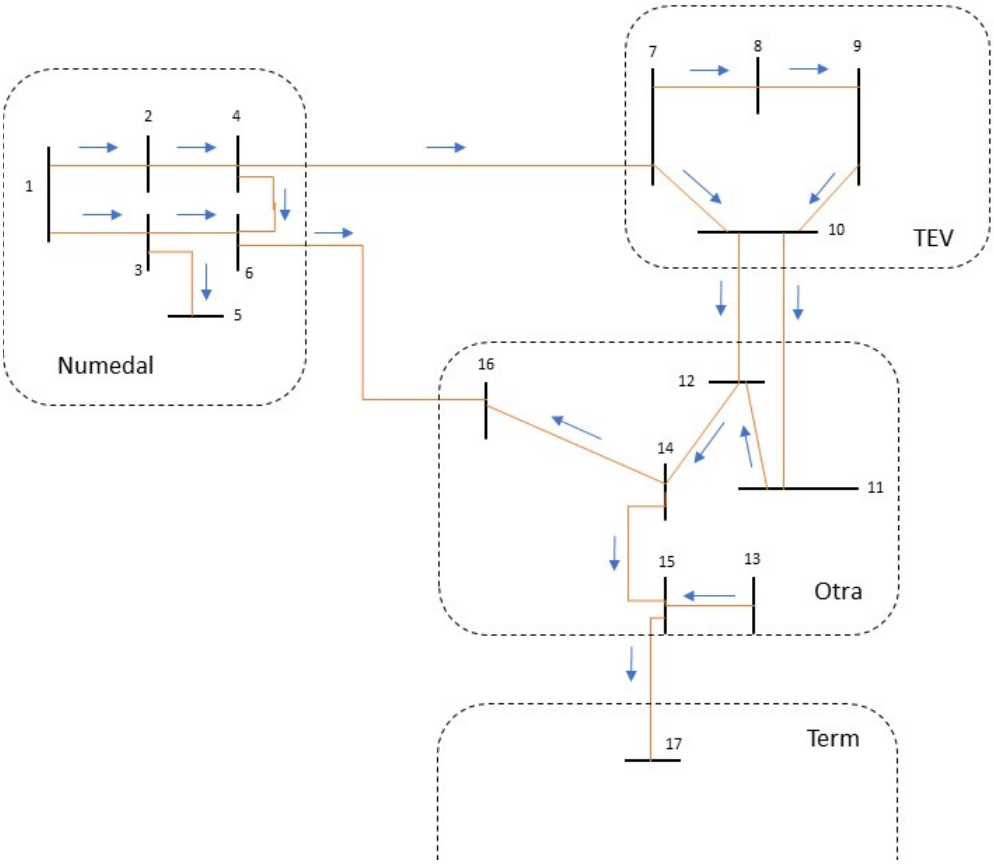

Figure 3.4: Grid of *4del*

However, *4del* does not contain the characteristics of the grid in terms of transmission lines and electrical capabilities of the generators and transformers. Therefore, a secondary data-set, *EMPS-nett*, is introduced to the model. *EMPS-nett* provides additional data for the system with information about base values for the transformers, generators and load. The values of the lines and buses are presented, thus making it possible to obtain the Y-bus matrix.

3.4 Grid Implementation

The implementation of the physical grid of the system is based on chapter 2, specifically section 2.5 and 2.6. To implement flow-based market coupling to the model, a thorough assessment of the available data is required, to accurately calculate the PTDF-matrix. The PTDF-values was calculated outside the model in order to keep simplicity in the program code, where the matrix is fed in similarly as the other in-put. An explanation of the specific steps of the implementation is presented below.

The grid has two different levels of voltage, and thus needs to be converted to a global p.u. for all lines, prior to the further calculation process. The lines within the zones are operating at 66 kV, while the transmission lines between the zones operate at 130 kV. The apparent power of the transformers, at 100 MVA form the base values that couple the high and medium voltage grid, as the reference voltage is set to 66 kV.

From the data-set *4del* and additional information from the data-set of EMPS-nett, an Y-matrix of the grid is calculated as in 2.12 prior the PTDF calculation process. Figure 3.4 has directions of the reference flow, where bus 14 in Otra is selected as the swing bus. This is further used in the calculations of the impedance matrix in equation 2.13. From equation 2.12 and 2.13 the detailed PTDF-matrix is obtained with equation 2.17.

In the system with four zones *4del*, the zone Term is interpreted as main Europe connected with a HVDC cable, and should thus not be considered for the flow based market coupling. The physical flow between the areas is calculated with constraints considering the bounds in the base case as ATC, as these are the only available limits.

Name	Line [nr. bus - nr. bus]	Capacity [MW]
Numedal - TEV	4 - 7	200.00
Numedal - Otra	6 - 16	100.00
TEV - Otra	10 - 11 & 10 - 12	200.00
Otra - Term	15 - 17	200.00

Table 3.1: Sections between areas

To connect the three zones, a generation shift key is used. A flat strategy was chosen in order to keep simplicity and low computational time, where the nodes in the zone where weighted equally within the area, and only calculated once prior to the simulation. Further, a similar GSK-strategy to the intended implementation of the TSO should prove beneficial, as the model is trying to imitate the market. The detailed, nodal PTDF-matrix was used to compute the zonal PTDF-matrix with the GSK as in equation 2.21. The sections between the zones are of interest, and the two transmission lines between TEV and Otra is considered as one section, as can be observed in table 3.1.

The zonal PTDF-matrix that is used in the simulations of the flow of power is calculated to be the following matrix, presented below. Columns with areas, and rows for the lines.

$$a_{i,j}^{area} = \begin{array}{c} \begin{matrix} \text{Numedal} & \text{TEV} & \text{Otra} \end{matrix} \\ \begin{bmatrix} 0.21020242 & -0.36917653 & -0.01212573 \\ 0.78979758 & 0.36917653 & 0.01212573 \\ 0.21020242 & 0.63082347 & -0.01212573 \end{bmatrix} \end{array} \begin{matrix} \text{Numedal - TEV} \\ \text{Numedal - Otra} \\ \text{TEV - Otra} \end{matrix}$$

The flow-based characteristics of the model need to be implemented with the PTDF-matrix and the net power of the zones. The physical flow from zone i to j in time step k is dependent on the net power in the areas. The net injected power consists of the power bought, the generated and pumped power, and the load and wind power for all zones corrected with the power distribution factor, PTDF. This could be simplified to the net transferred power out an area, $P_{net\ inj}$.

The implementation of the grid with flow based market coupling will be as follows, derived from equation 2.19 and 2.20, constrained by the transfer capacities in the ATC of the original model.

The flow from i to j in time-step k is equal to the sum the line's PTDF-matrix elements $a^{a}_{i,\ j}$, where $a^{a} = a^{area}$ from the presented matrix above, multiplied with the corresponding area's net injected power. The net injected power is modeled as the the power with a reference out of the area. The power is distinguished in f and t, as the flow-based variable between the hydro areas, $\mathcal{A}_{\mathcal{H}}$, and the variable for transmission to thermal areas, $\mathcal{A}_{\mathcal{T}}$. The sum of $f_{a,h,k}$ is the flow of power from the area, a, to all other areas in $\mathcal{A}_{\mathcal{H}}$, h. The sum of transmitted power from the area a, to the other areas in $\mathcal{A}_{\mathcal{T}}$, l is divided into two variables. $t_{a,l,k}$ is constrained at zero, and does therefore need the subtracted with the opposite directed flow, including a transmission loss.

Physical flow

$$f_{i,j,k} = \sum_{a \in \mathcal{A}_\mathcal{H}} a^a_{i,j} \cdot \left(\sum_{h \in \mathcal{A}_\mathcal{H}} f_{a,h,k} + \sum_{l \in \mathcal{A}_\mathcal{T}} t_{a,l,k} - t_{l,a,k} \cdot (1 - \mathcal{T}^{loss}_{l,a}) \right)$$
$$i,\ j \in \mathcal{A}_\mathcal{H}, \quad k \in \mathcal{K}_t \tag{3.12}$$

Transfer capacity, flow based zones

$$-\mathcal{T}^{cap}_{i,j} \leq f_{i,j,k} \leq \mathcal{T}^{cap}_{i,j}, \qquad i,\ j \in \mathcal{A}_\mathcal{H} \tag{3.13}$$

The implementations lead to some necessary changes to the model. The parameter $a^{area}_{i,j}$ is included in the list of parameters. The set $\mathcal{A}$ has been divided into the subsets $\mathcal{A}_\mathcal{H}$ and $\mathcal{A}_\mathcal{T}$, where the three hydro areas are located in subset $\mathcal{A}_\mathcal{H}$ and the thermal area, Term, is in $\mathcal{A}_\mathcal{T}$. The model should be scalable with these changes, to handle larger data-sets provided that the grid data is available.

Negative prices can in be seen in markets with a high penetration of intermittent RES, which in a situation where production is in excess, prices may drop below zero. Continental Europe have seen this phenomenon happen due to high levels of production in wind and solar power [46]. However, in an area dominated by power production from hydro, where the water can be stored and used at a later stage. Negative prices will thus not be realistic in a model where the the inflow can be dealt with, and there are no major penalties imposed.

Flow-based market coupling may cause negative prices in an area due to congestion, where the binding constraints from the lines with PTDF cause negative dual values in the constraint 3.4. To avoid overproduction of

power, resulting in negative prices, an additional variable is introduced. $y_{a,k}^{slack}$ will act as slack variable in 3.4 to evict redundant power, and ensure a positive dual value [21].

However, this variable also needs to be controlled, to avoid drainage of the reservoirs, and a parameter for a penalty, $\mathcal{P}^{slack}$, is therefore imposed on this variable in the objective function 3.1. The value of the penalty is set in the same magnitude to the other penalties in the model to ensure that it does not dominate the optimization.

The complete model with the implementation of flow-based market coupling could be observed in the appendix.

Chapter 4

Results

A selection of the results from the base case will be presented in this section, alongside with the results from flow-based market coupling. The original version of PriMod, with transport modeling of the power, is referred to as the base case. The presented results are area prices, stored hydro, and power flow in the transmission lines, for a specific year of inflow and load.

The duration of the simulation was set to one calendar year. In the simulation each of the 52 weeks were divided into 168 time-steps, totaling 8736 time-steps of the simulation.

4.1 Pricing

The prices presented in table 4.1 are the median and average prices for the *4del* system for the simulated 52 weeks.

FBMC	Numedal [€/MWh]	Otra [€/MWh]	Term [€/MWh]	TEV [€/MWh]
Average	52.10	52.10	54.13	52.10
Median	33.52	33.52	34.92	33.52
Base case	Numedal [€/MWh]	Otra [€/MWh]	Term [€/MWh]	TEV [€/MWh]
Average	52.95	53.39	55.44	52.59
Median	35.32	35.45	36.93	34.75

Table 4.1: Average and median prices for FBMC and base case simulations

To assess how flow-based market coupling affects the prices of the system, the prices for all time-steps in week 1 are plotted in the figures 4.1, 4.2, 4.3 and 4.4, for the four areas in *4del*.

The scope of one week was chosen to showcase the weekly price-structure, and to illustrate in what situations that price differences occurred. In the plots, the simulation with FBMC is plotted with the base case for the same area. Week 1 was chosen for this plot to ensure equal initial reservoirs.

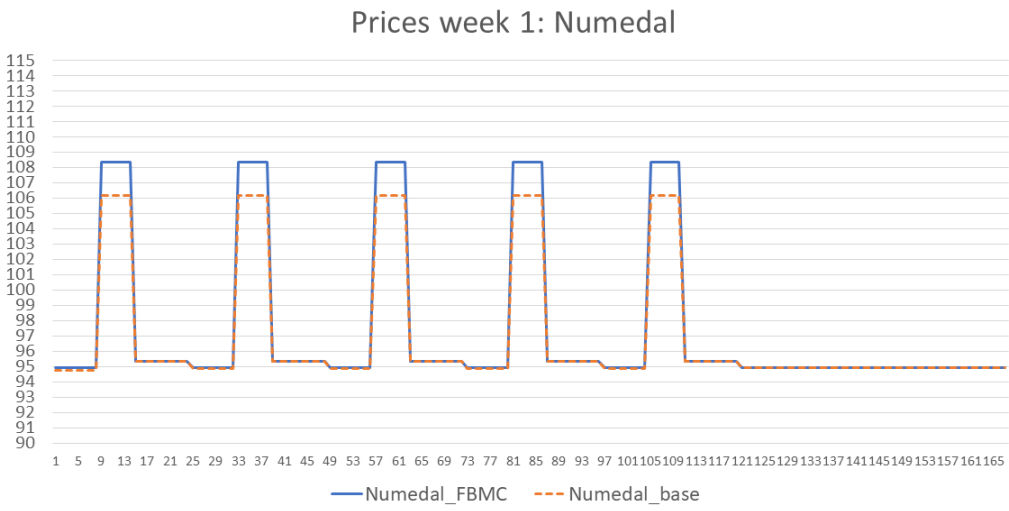

Figure 4.1: Prices at Numedal for week 1 [€/MWh]

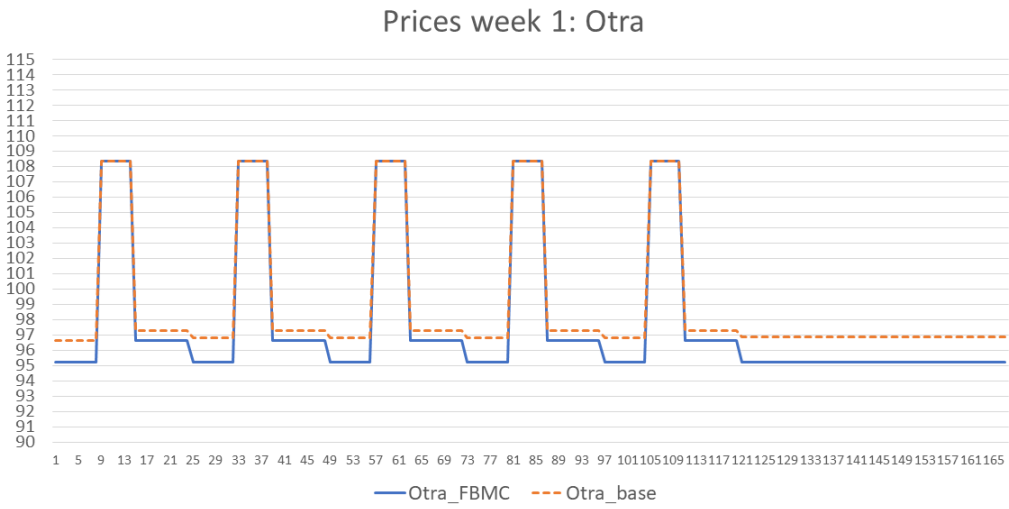

Figure 4.2: Prices at Otra for week 1 [€/MWh]

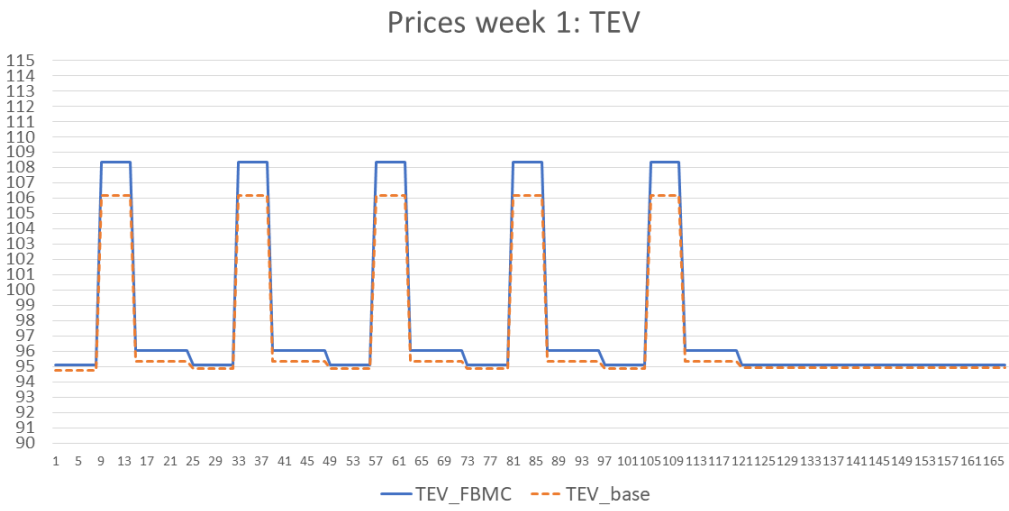

Figure 4.3: Prices at TEV for week 1 [€/MWh]

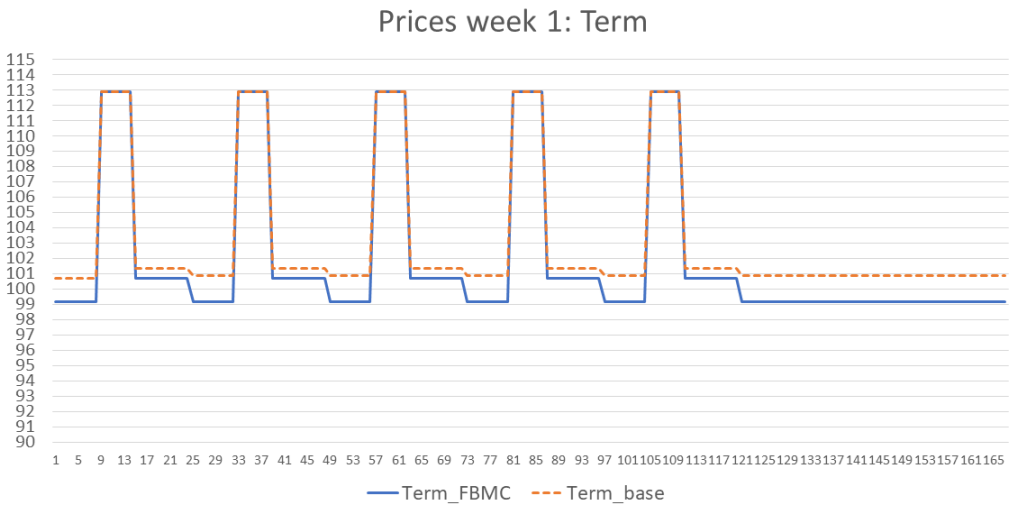

Figure 4.4: Prices at Term for week 1 [€/MWh]

4.2 Stored Hydro

The stored hydro in reservoirs in the three hydro areas is presented below in figure 4.5 and 4.6. The volume of stored water in the figures is stacked in order to interpret the situation of the whole system over the simulated year. The Reservoir levels are included in the results, due to their effect on future prices in the system. The values of the reservoirs are presented in table 4.2.

	Start reservoir [Mm^3]	End reservoir [Mm^3]
FBMC total	2768.87	2048.85
Numedal	605.345	120.99
Otra	1265.29	1308.11
TEV	898.235	619.75
Base case total	2768.87	2079.48
Numedal	605.345	114.11
Otra	1265.29	1301.64
TEV	898.235	663.72

Table 4.2: Start and end reservoirs for FBMC and the base case.

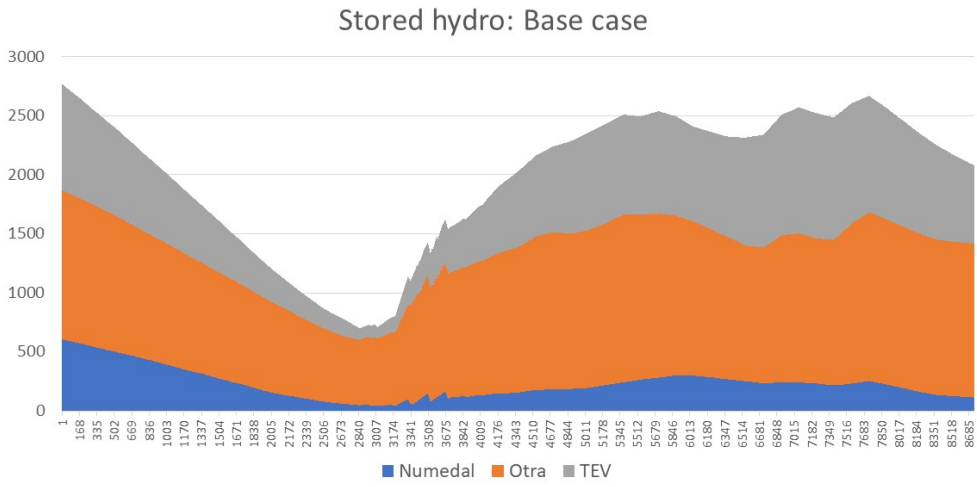

Figure 4.5: Accumulated hydro [Mm^3] for all time-steps in the base case simulation, 168 steps a week

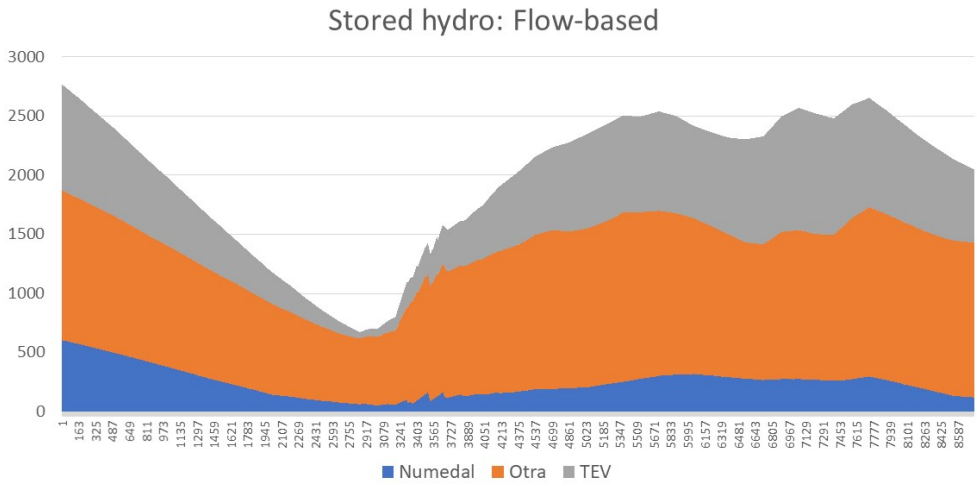

Figure 4.6: Accumulated hydro [Mm^3] for all time-steps in the flow-based simulation, 168 steps a week

4.3 Power Flow

The physical flow of power is presented in this section. The results illustrate a comparison of the FMBC and the base case. The plotted results show the direction and magnitude for all time-steps in the 52 simulated weeks.

The figures must be read as for positive values, the flow is directed at the second area in the name of the line, i.e. referenced as receiving end of the line. Similarly, negative values indicate a flow towards the first area in the name of the transmission line.

The line Term - Otra is a HVDC line. Thus, it does not contain the characteristic of the other flow-based transmission lines.

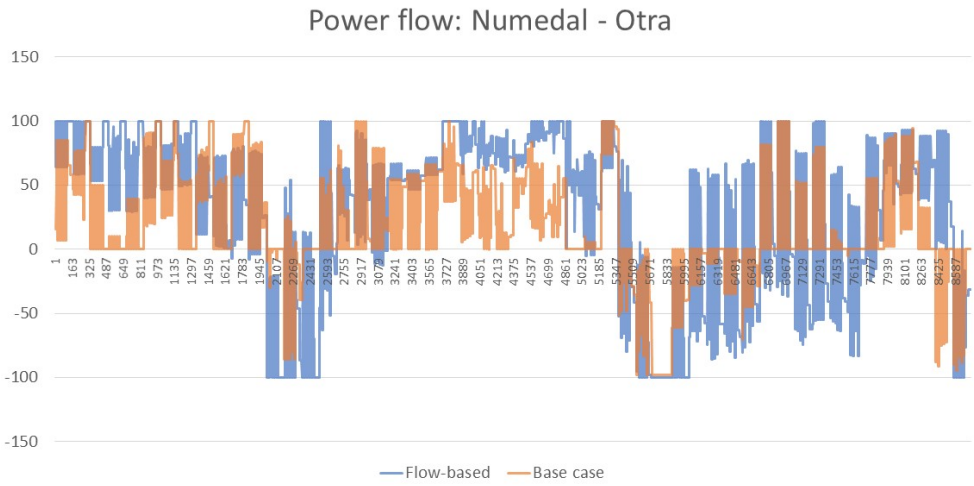

Figure 4.7: Power transfer Numedal - Otra [MW], FBMC and base case 168 steps a week

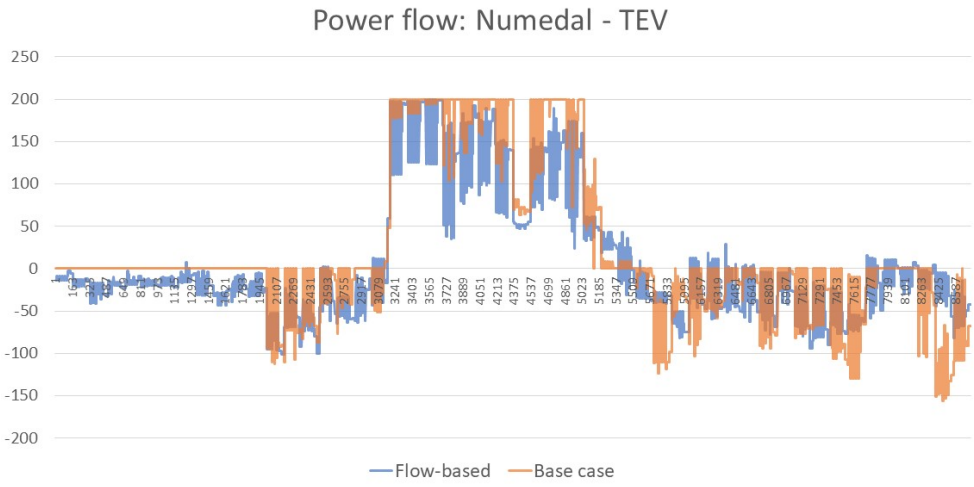

Figure 4.8: Power transfer Numedal - TEV [MW], FBMC and base case 168 steps a week

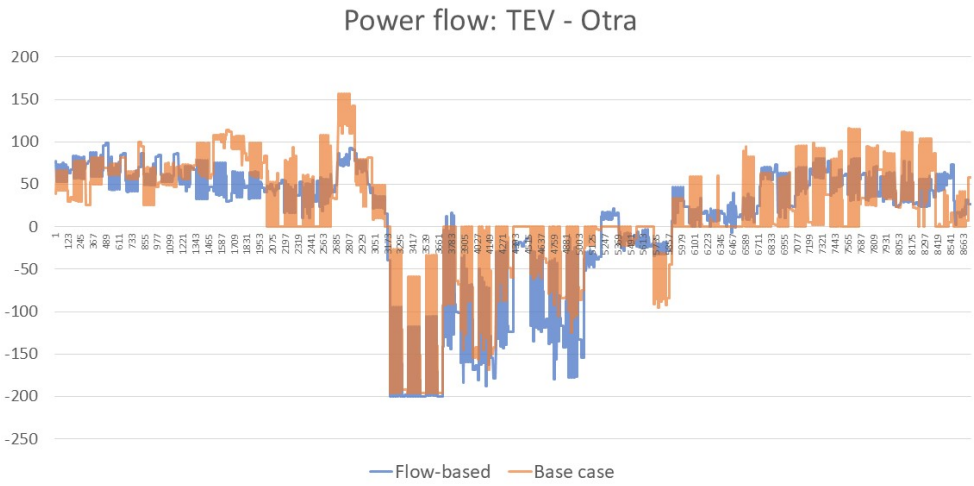

Figure 4.9: Power transfer TEV - Otra [MW], FBMC and base case 168 steps a week

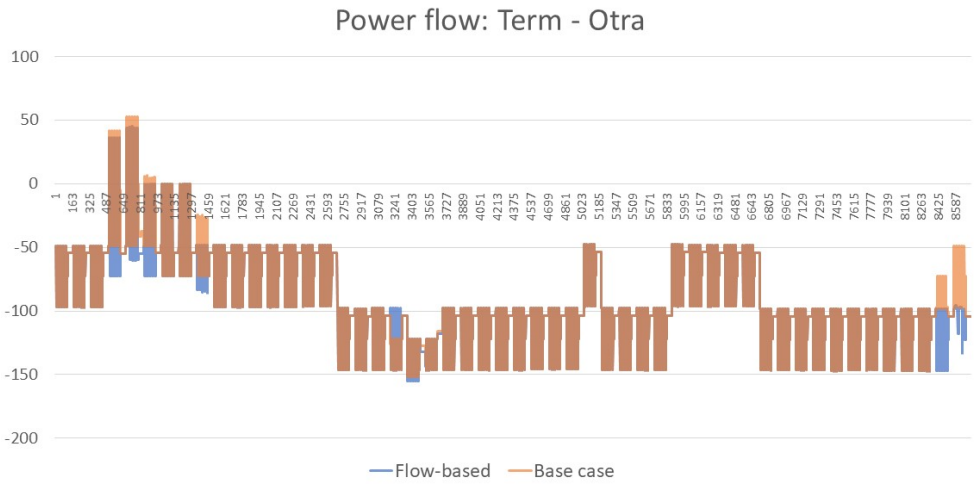

Figure 4.10: Power transfer Term - Otra [MW], FBMC and base case 168 steps a week

Chapter 5

Discussion and Analysis

This chapter will discuss the findings of the simulation and furthermore connect and analyze the results from chapter 4. The first sections will provide a broad perspective to the results, while later in the chapter, more specific analyses will be provided.

5.1 Physical Flow

The fundamental change in the results of the simulations are the differences in flow. In this section the alterations in the systems flow of power, due to FBMC, will be assessed to show how flow-based market coupling affects the physical flow in the grid. In this section the base case and FBMC solution is compared with an uncapped simulation, where the maximum capacities of the lines are removed, in order to find an optimal solution. This will cause equal prices in the whole flow-based system, that will be explained further in section 5.4.

An analysis on the the three lines for the flow-based market coupling is plotted with duration curves. Both the FBMC and base case are plotted

with the uncapped simulation. For this case, the maximum capacities of the lines are removed, in order to find an optimal solution. The three lines are observed in figure 5.1, 5.2 and 5.3. The duration curves are the results presented in 4.3, in order of magnitude for all the 8736 steps of the simulation.

As observed, the uncapped simulation exceeds the maximum capacity of the lines as expected. For those occurrences the base case and FBMC are not able to follow the uncapped simulations, due to their restrictions. The first instance of comparison is after the uncapped simulation crosses the threshold of the capacities.

The FBMC solution outperforms the base case in terms of being able to follow the uncapped solution, when possible. In table 5.1, the average difference between the two simulations and the uncapped solution is presented.

Line	FBMC [MW]	Base case [MW]
Numedal - Otra	4.96	33.89
Numedal - TEV	2.57	22.60
TEV - Otra	2.13	20.97

Table 5.1: Average difference between actual flow and uncapped solution

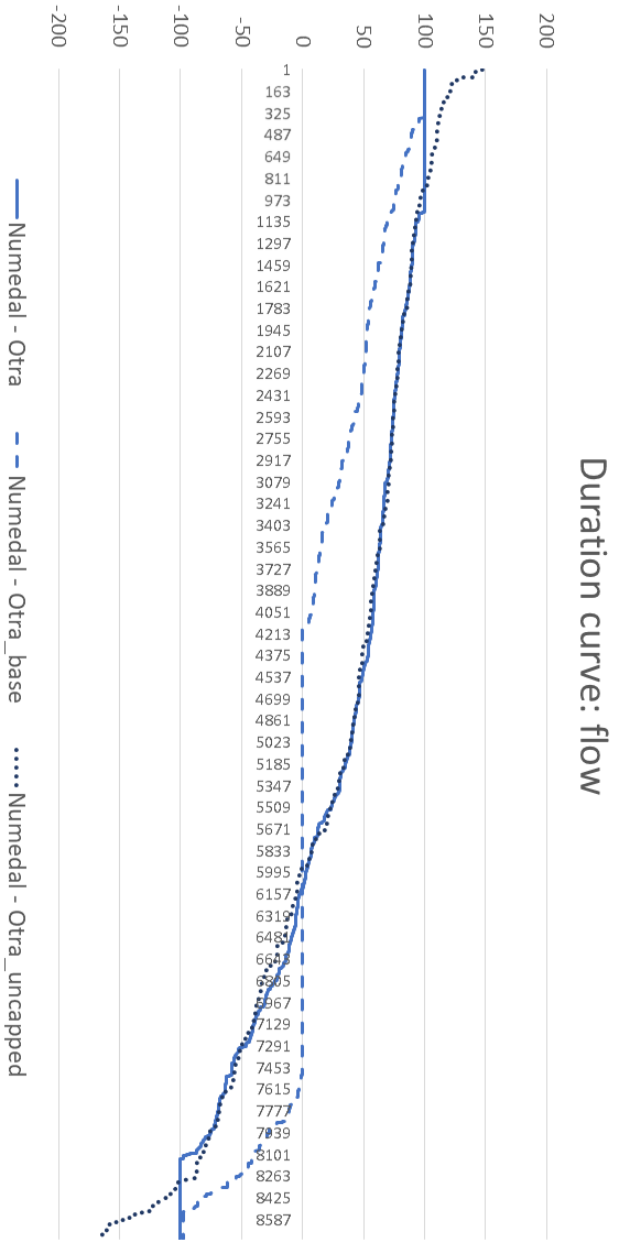

Figure 5.1: Duration curve flow of power between Numedal and Otra, transferred power on y-axis [MW], for all 8736 time-steps.

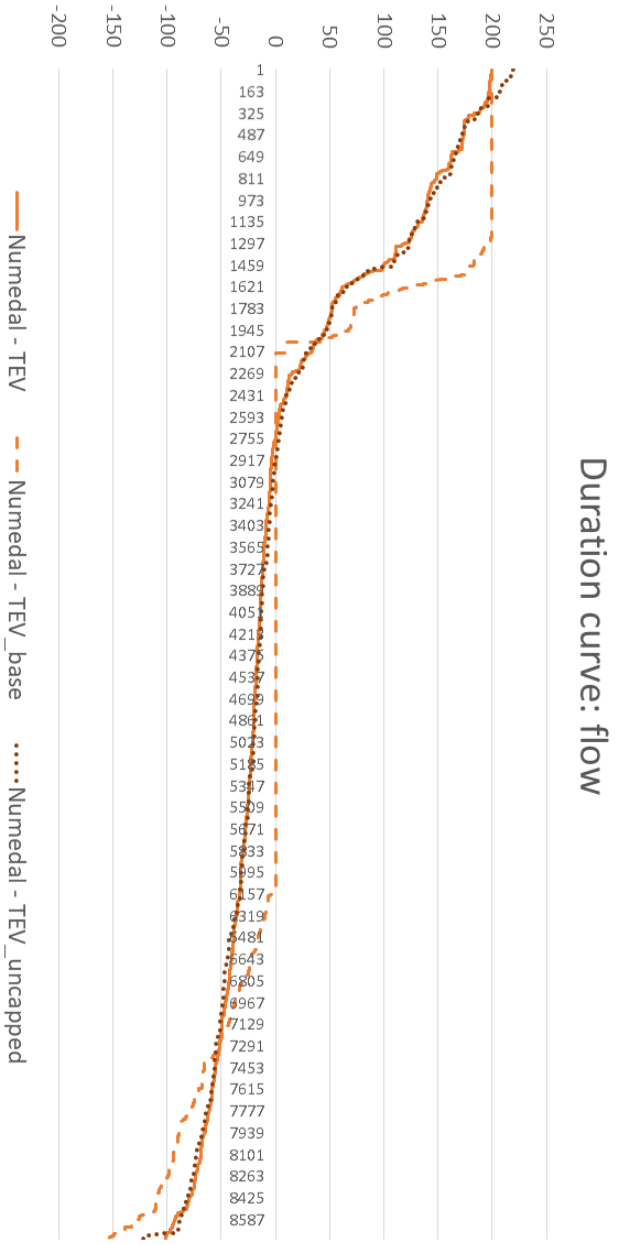

Figure 5.2: Duration curve flow of power between Numedal and TEV, transferred power on y-axis [MW], for all 8736 time-steps.

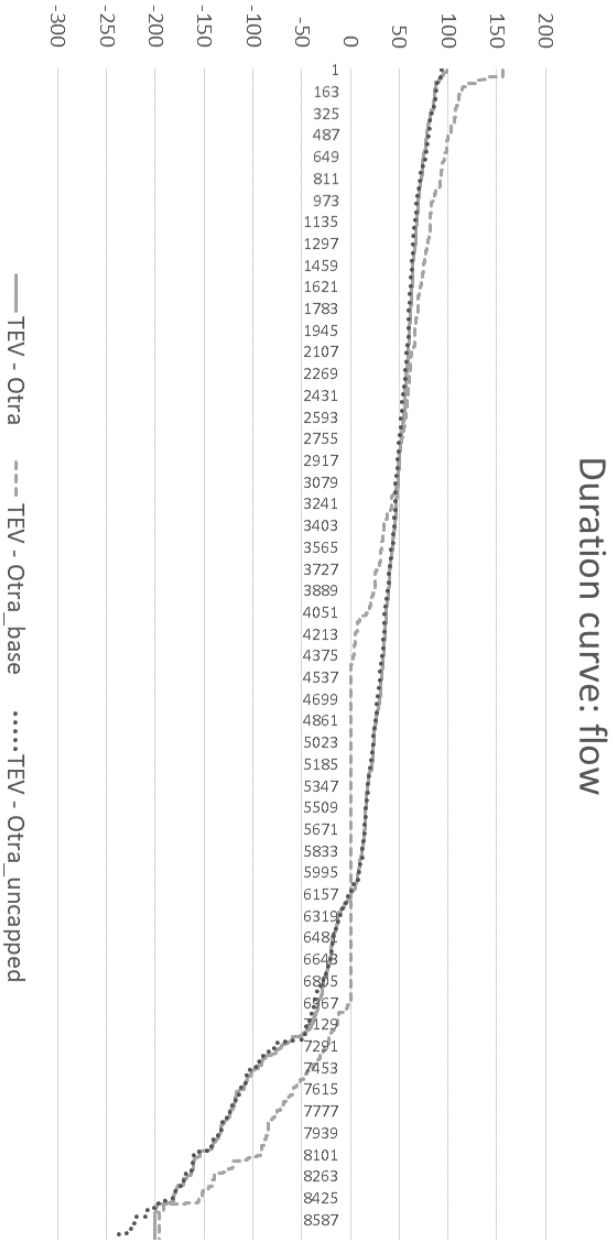

Figure 5.3: Duration curve flow of power between TEV and Otra, transferred power on y-axis [MW], for all 8736 time-steps.

To further study the flow of power in the system, the flow at the area Numedal is analyzed. The flow in the lines Numedal - Otra and Numedal - TEV in figure 5.1 and 5.2 is illustrated with a scatter plot, to comprehend the combination of the simultaneous flow in the two lines.

In the base case Numedal will exclusively act as an import area or export area, for a given time-step. This is observed in figure 5.4. If Numedal is the lowest priced area, the point of the flow will be within the first quadrant, and similarly if it is the area with highest prices, it will import from both Otra and TEV, where the point will be in the third quadrant. However, if Numedal is priced equally to the low-priced zone, or between the extremities, there will be no flow between the two lowest priced zones. This is observed along the x- and y-axis.

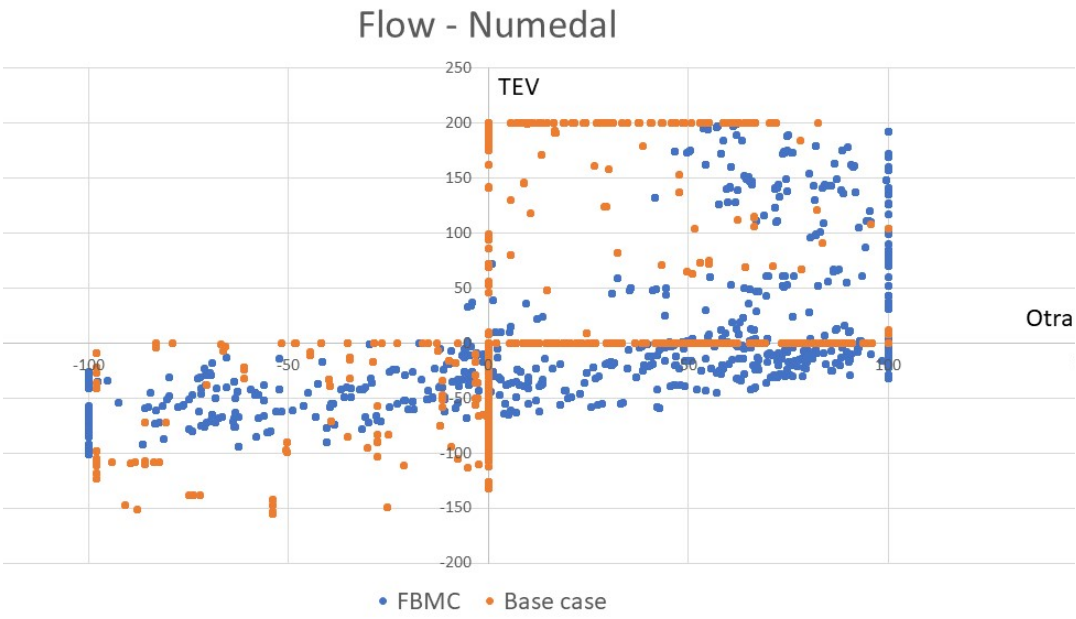

Figure 5.4: Flow at Numedal [MW]

The pattern for the flow-based simulations is quite different from the base case. The difference in the flow lies in the coupling of the zones. The conventional coupling considers the neighbouring area, and if an opportunity of arbitrage exists through transmission of power, the power will be transferred to the relevant area. The flow-based market coupling may send its power through another area to reach the destination zone. This is the essence of the PTDF-matrix, as it describes how the power is distributed in the network. The elements in the PTDF-matrix $a^{Numedal}_{Numedal,TEV} = 0.21020242$ and $a^{Numedal}_{Numedal,Otra} = 0.78979758$, presented in section 3.4, indicate how much of an increase in injected power at Numedal affects the the lines to other Otra and TEV. Thus, import and export may coincide in one time-step for the flow-based solution. In the second quadrant of figure 5.4 TEV is transferring power through Numedal to Otra in accordance with the PTDF-matrix, where the solver finds the optimal solution. This phenomenon is further explained in section 5.4.

This concept may lead to less congestion of the lines, due to the altered flow of power. This is observed in figure 5.2, which is on the y-axis in figure 5.4. However, the altered flow causes an increase in time-steps with congestion on the line Numedal - Otra and need to be seen in the context of the prices presented in section 5.2. The number of steps with congested lines are presented in table 5.2, where the level of congestion with FBMC is lower than in the base case.

There has been a shift in congestion where the Numedal - Otra is the constraining line in the system. This could be explained by the maximum capacity of the transmission line in table 3.1, where Numedal - Otra has half the capacity of the other lines. Moreover, the changed levels of congestion must be seen in context of the prices presented in section 5.2 with figure

5.5 and 5.6.

The slightly lower levels of congestion, are promising results, when taken into account that the base case is less restricted than the FBMC due to the lack of the NTC. The ATC should be within the domain of the FBMC, while in this simulation it surrounds the FBMC domain.

	Numedal - TEV [steps]	Numedal - Otra [steps]	Total [steps]
Base case	1256	570	1826
FBMC	40	1640	1680

Table 5.2: Congestion in lines

5.2 Price Structure

Market prices serve as an important indicator of how well-functioning an electrical market is operating. In figure 5.5 and 5.6, the prices in neighbouring areas and the flow in the transmission line are studied.

As previously mentioned, the prices are calculated as the dual values of the power balance in an area. The flow is one of the main contributors to the total power in an area, and acts as a regulator to even out prices.

As described in section 3.2, the water values are determined by the dual of the reservoir balance in equation 3.2. From the results in section 4.2, the observation is that the differences in reservoirs are small. The base case has a decrease of 24.90%, while the simulations with FBMC had 26.00% in stored hydro. This difference can not be accounted as significant changes between the water values in the base case and the flow-based simulations.

A comparison between the base case and FBMC simulation can therefore be justified as the projected future profit of stored hydro, and should be approximately equal. However, it must be noted that the difference in stored volume, Mm^3, does not necessarily represent the stored power in MWh, as the relative height, and efficiency curves of the production units differ between the plants and reservoirs.

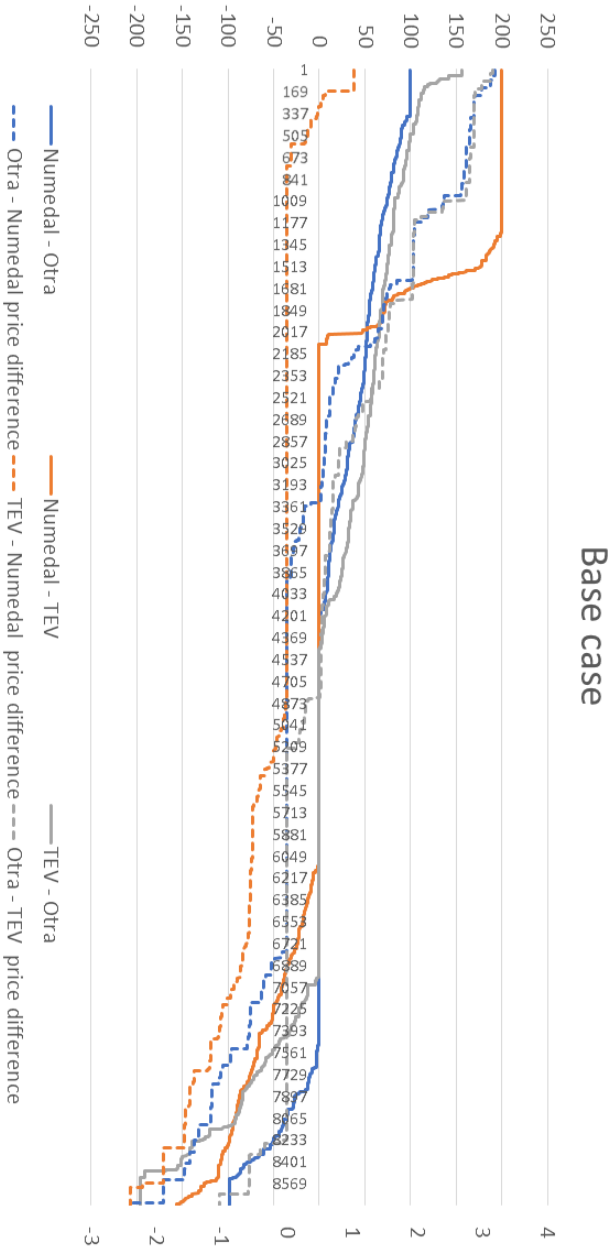

Figure 5.5: Duration curve base case, transferred power on left y-axis [MW], price difference on the right y-axis [€/MWh]. For all 8736 time-steps.

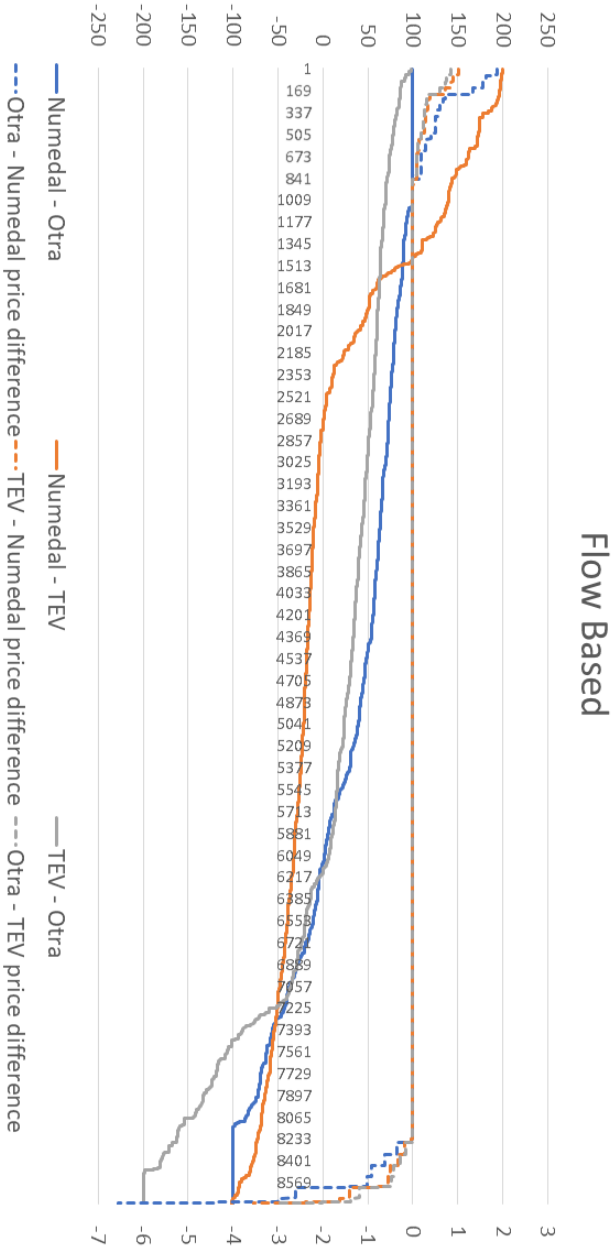

Figure 5.6: Duration curve flow-based market coupling, transferred power on left y-axis [MW], price difference on the right y-axis [€/MWh]. For all 8736 time-steps.

Convergence	Time-steps	Percent of simulated period
Base case	1368	15.61 %
FBMC	7028	80.45 %

Table 5.3: Convergence of prices in all areas during the simulation

There is a significant change in number of time-steps that all areas are converging to an equal price. As observed in the duration curves 5.5 and 5.6, the flow-based simulation, has considerably many more time-steps at zero price difference for all areas compared with the base case simulation. Due to potential numerical errors, the limit for convergence is set to price differences less than 10^{-4} €/MWh.

The values of convergence are presented in table 5.3. The increase in convergence is seen in the context of section 5.1, where the simulation with FBMC implemented, has a much more similar behaviour to the uncapped solution, than the base case. As previously stated, the uncapped solution will have equal prices for all time-steps. Thus, a high resemblance to this solution will cause a high level of converging prices [23].

5.3 Domain of Solution

An essential part of understanding the differences between flow-based market coupling and conventional market coupling lies with the domain of the solutions. The solution of the power flow will be within a different domain than that of the base case, that uses the ATC/NTC domain discussed, in section 2.5.

The boundaries of the PTDF is assumed to have a larger domain than the ATC of the base case. However, there is a lack of information that could

indicate the differences in the ATC and NTC of the model. The capacity of the lines in the base case must be considered as the ATC for the base case, and as the NTC for the FBMC solution, due to the absence of a differentiation between the two. Thats why the FBMC solution domain is smaller than the ATC domain in figure 5.7. In this case the ATC model will overestimate the transmission capability of the system.

A domain of the net power in two areas could be illustrated in order to observe the constraints that form the possible outcome of two of the areas. The constraints in the power balance for physical flow in 3.12 form this domain and can be plotted as the following.

$$x_{i,j}^{Numedal} = \frac{\mathcal{T}_{i,j}^{cap}}{a_{i,j}^{Numedal}} \qquad y_{i,j}^{TEV} = \frac{\mathcal{T}_{i,j}^{cap}}{a_{i,j}^{TEV}} \tag{5.1}$$

The constraint will be the line through the points $(x_{i,j}^{Numedal},\ 0)$ and $(0,\ y_{i,j}^{TEV})$. This is applied for all the transmission lines, which forms the domain of the net power of the two areas, Numedal and TEV. The net power of a node is defined here as the produced power minus the load in the area, or similarly as the sum of outwards directed power from an area.

$$P_{net}^{area} = \sum_{a \in other\ areas} f_{area,a} \tag{5.2}$$

The domain of the net position of power at Numedal and TEV, in x- and y-direction respectively, can be observed in figure 5.7. The constraints for the net position of Numedal and TEV can be read as:

Constraint	Line
1. Top left	TEV - Numedal
2. Top right	TEV - Otra
3. Right	Numedal - Otra
4. Bottom right	Numedal - TEV
5. Bottom left	Otra - TEV
6. Left	Otra - Numedal

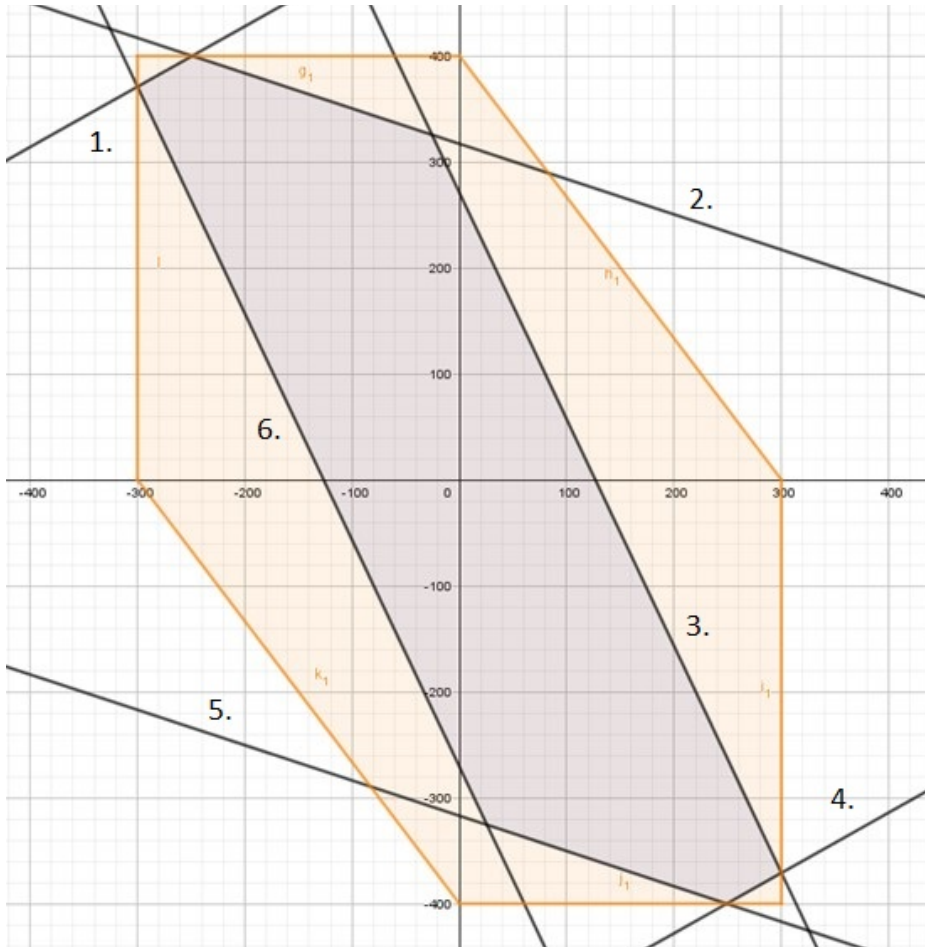

Figure 5.7: Domain of $P_{net\ inj}$ at Numedal (x-axis) and TEV (y-axis) for flow based solution (blue), and base case (orange)

The net power for Numedal and TEV are plotted for all time-steps for the simulated year, 8736 points in the scatter-plot 5.8.

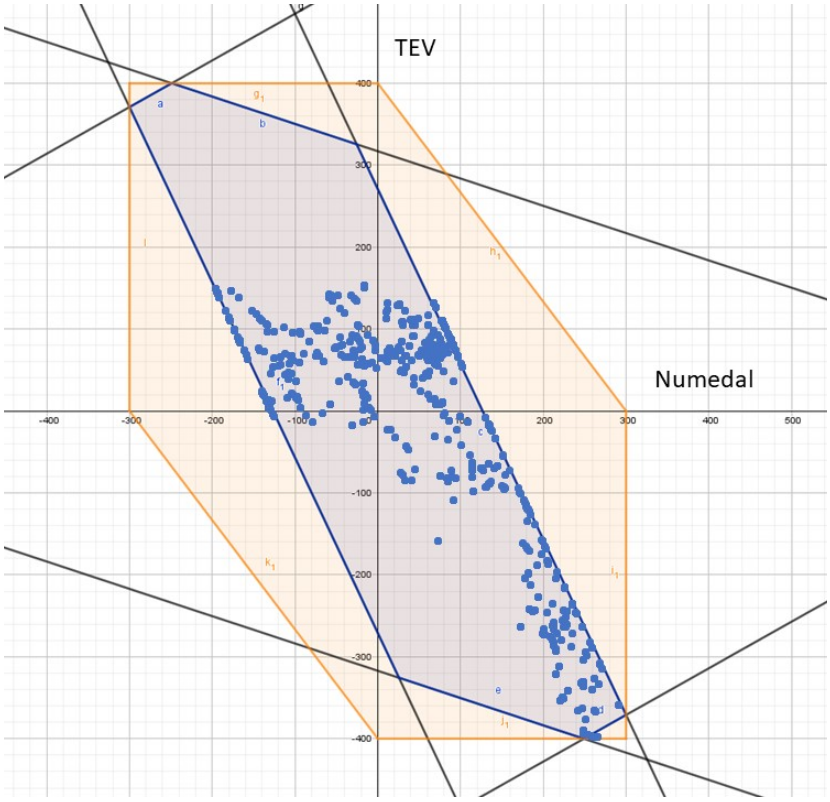

Figure 5.8: Net power at Numedal and TEV, with PTDF restrictions (blue), and the domain of the NTC (yellow)

Some interesting observations could be drawn from the figure, where the most striking is where the constraints are binding. Except from some points, the binding constraints are the right and left, bound by the line Numedal and Otra, in the reference direction on the right, and opposite of the reference to the left. From this observation, and table 5.2 it can be deduced that the line Numedal - Otra is the most constraining line in the system.

5.4 Detailed Flow

To further analyze how flow-based market coupling affects an electrical grid, a detailed illustration of a single time step is assessed.

Applying a system without line capacity limits creates a benchmark for comparison with the implemented solution. In time step $t = 1$ the water values of both simulations are equal, and this time-step is therefore chosen, as the reservoir levels may differ later in the simulation due to different patterns of discharging of the hydro.

In figure 5.9 below, key values are presented, both for the solution without limits of capacity $No\ cap$, and for the implemented FBMC solution with the limits of the transmission lines equal to the ATC of the primary model, Cap.

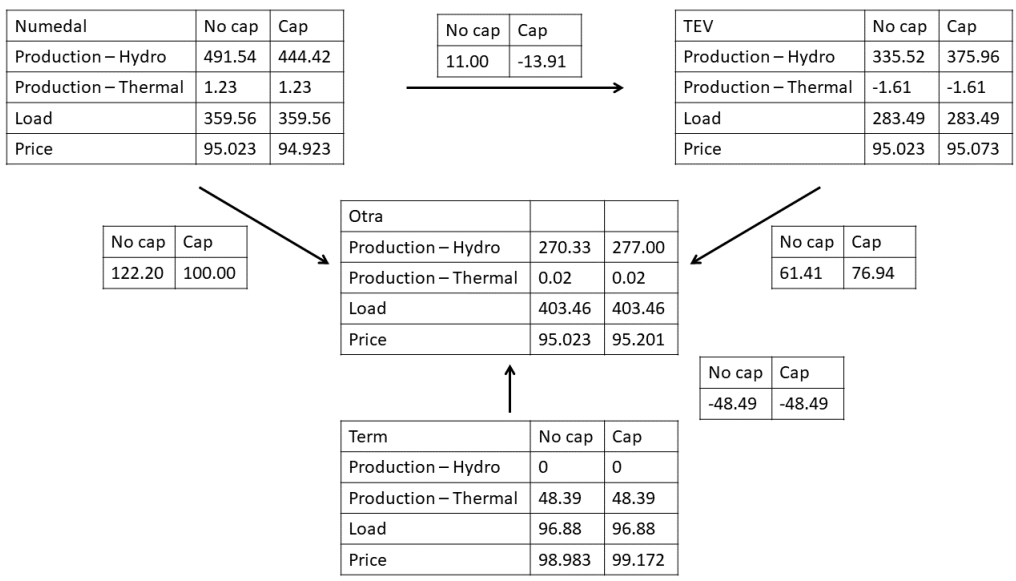

Figure 5.9: Prices in [€/MWh], and load, production and flow in [MW]

In the $No\ cap$ simulation, all hydro areas are priced equally due to the fact that the solver will try to minimize the costs, which in turn will provide the socio-economic optimum, as described in section 2.2.2. The prices $No\ cap$ are calculated similarly to the system prices at NordPool, from unconstrained transmission lines in the market clearing.

The thermal production in the three hydro areas, Numedal, TEV and Otra, contributes only to a small extent to the total power production. The thermal production in TEV is negative for both the $No\ cap$ and Cap simulations, due to the modeling of thermal production and elastic demand, described in section 3.3, as the prices permits profitable production in the industry located in TEV. The additional demand is described as negative thermal production.

After the introduction of the limits in the Cap simulation, a change is observed in the flow between the FBMC areas. Under the $No\ cap$ simulation, the flow of the line Numedal - Otra was higher than the actual capacity of the line. Thus, it required correction down to 100 MW. The intuitive understanding of arbitrage, is to produce power in the cheaper area and sell as much as possible to a higher price. As a result, the line is congested between the two areas Numedal and Otra.

In the conventional ATC market coupling the flow of power always goes from the lower priced area to a higher level of cost. However, in this example the prices in Numedal and TEV do not follow this pattern. Even though the cost of power in Numedal is lower than in TEV, the power flows from TEV to Numedal. This is a very interesting result and needs further explanation.

The constraints from the PTDF are limiting the solution, and the constraints Otra, Numedal and Otra, TEV are the two constraints affecting the solution. Further, the solution could be graphically represented as of the figure 5.7 in section 5.3, as a point P = (86.09, 90.85) from the calculations of net power at Numedal and TEV as the sum of the flow directed out of the area.

$$P_{net}^{Numedal} = f_{Numedal,\ TEV} + f_{Numedal,\ Otra} = 86.09\ MW$$

$$P_{net}^{TEV} = f_{TEV,\ Numedal} + f_{TEV,\ Otra} = 90.85\ MW$$

This point will be laying on the limit constrained by the PTDF of Numedal - Otra.

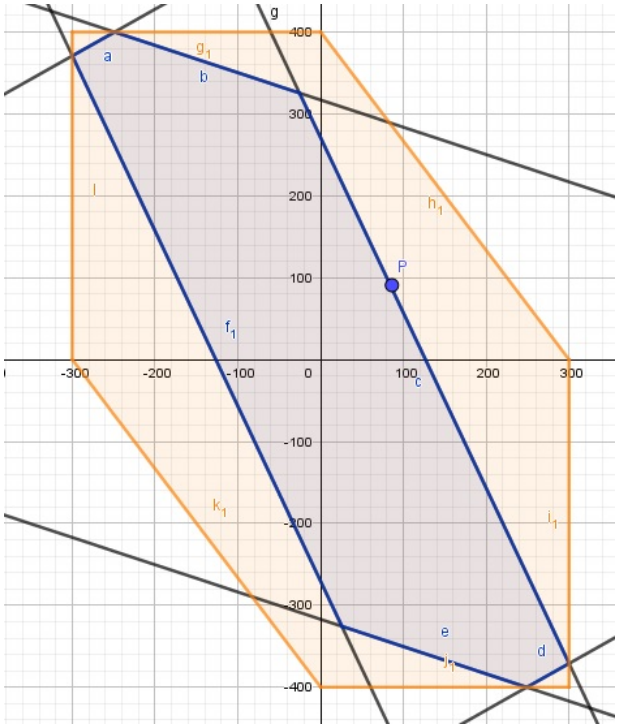

Figure 5.10: Point P, on the right constraint of the net power for Numedal (x-axis) and TEV (y-axis)

The concept of flow of power from a high cost area, to a lower cost area is described as ”non-intuitive” by CWE [3]. ATC market coupling provides the conventional explicit market coupling, with cross-border arbitrage. Intuitive flows go from a low cost zones to high priced zones is the intuitive way of clearing the market. However, if the system is solved as a whole, and the objective of the optimization is to maximize the total social welfare, the flow of power may at some stages of operation be ”non-intuitive” in the implicit market clearing.

The constraint for flow in the optimization model, is constrained for the instances of Otra - Numedal and Otra - TEV. The duals for these two constraints are -0.07587 and -0.07616. This indicates that the economic losses for constraints in the lines are close to equal, due to the characteristics of dual values in the solution of an optimization problem. This could further be used to compute the cost for congested lines, coupled with the PTDF-matrix [21].

	No cap	Cap	Base case
Numedal	95.02	94.92	94.73
TEV	95.02	95.07	94.73
Otra	95.02	95.20	96.66
Term	98.98	99.17	100.66

Table 5.4: Prices step 1, [€/MWh]

The ”non-intuitive” market coupling provides a solution within the limits that is closer to converging on price than the conventional ATC market coupling. The prices at time-step 1 are presented in table 5.4.

To enable the system to reach the best possible solution within the limits on capacity, the power must therefore flow from TEV to Numedal, despite the negative differences in price.

5.5 Financial Consequences

The economic consequences of implementing FBMC in the Nordic power market are still unknown. However, some predictions based on the results of the simulations in chapter 4, the analyses and observations made in this chapter, and the financial instruments explained section 2.2, can be made. The financial market and the operational physical markets, day-ahead, and intra-day will operate similarly as the current market structure due to that prices are the driving factor in the markets, not the allocation mechanism.

Implicit market clearing through FBMC will make predictions for future earnings more complicated due to changed patterns of flow. ”Non-intuitive” flows of power as discussed in section 5.4, may decrease some producers profits under certain circumstances. In table 5.5, the flow towards the lower priced area is presented as a percentage of the total number of time-steps. To account for numerical errors, and insignificant values, the price differences less than 10^{-4} €/MWh are considered zero.

Numedal import power in 6.85% of the time-steps, when the price is lower than in the connected area. Considering that the prices are equal in 80.45% of the simulated time-steps, ”non-intuitive” import accounts for over a third of the time-steps with difference in prices. The opportunity to profit from arbitrage is lost for the producers in the low-priced area for those time-steps.

	Numedal [%]	TEV [%]	Otra [%]
Numedal - TEV	6.85	0.00	-
Numedal - Otra	0.00	-	1.56
TEV - Otra	-	1.72	3.48
Total	6.85	1.72	5.04

Table 5.5: "Non-intuitive" flow between areas [% of total 8736 time-steps]

The line Numedal - Otra has a considerably lower amount of "non-intuitive" flow in either direction. This must be seen in the context of figure 5.8, and the discussion in section 5.3. If Numedal - Otra is the most congested line, it is likely that the line usually has the highest price difference, thus highest allowed flow.

For a depreciated hydro plant, with low variable cost for production, changed patterns of flow is not crucial, but the scheduling of production needs to be revised, and account for these circumstances. However, investments in new, intermittent, renewable sources of power may be affected to a higher degree, as it requires selling the power at a higher price to break-even, and producers are not able to control the production in the same fashion as hydro-producers. The consequences of this may be a higher dependence of PPAs to fix the selling price to a level that the producer is able to operate at.

Converging prices may disturb the market for EPADs due to the changed structure of prices. In the simulations, the converging prices reached a level of 80.45% from 15.61% in the base case, presented in table 5.3. The allocation is still not perfect, thus allowing the EPADs to still be a trade-able product, but will occur on fewer occasions.

The observations made in section 5.1, suggest that the level of congestion

may be lower with flow-based market coupling. The lower levels of congestion, will lead to savings for the TSO and DSO, in terms of a reduction in investments in new lines and upgrading of the existing. Between 2017 and 2021, the Norwegian TSO, Statnett estimates an investment of 40-50 Billion NOK in upgrading and development of the grid [40]. Thus, the savings from a less congested grid will be considerable.

Chapter 6

Conclusion & Further work

Implementation of flow-based market coupling in the model PriMod is demonstrated and verified on a small-scale test system, including the associated PTDF-matrix for the *4del* system. The results are presented and discussed, where the key findings were:

- The level of congestion in the lines is somewhat lower with FBMC, and the most congested line has changed from Numedal - TEV, to Numedal - Otra, in regard of the base case with the transport modeling of the lines.

- The structure of the pricing has changed significantly. The prices converge in 80.45% of the steps, compared to 15.61% in the base case.

- Due to an improved allocation of power, the median and average prices are lower for the FBMC than the base case.

- The system acts ”non-intuitive” in a significant amount of time-steps. Numedal imports power in 6.85% of the simulated time-steps despite

a higher market price in the exporting area. For TEV and Otra the numbers are 1.72% and 5.04%.

The results have some of the characteristics that could be expected, and thus be correctly implemented. However, this must be validated, and some areas that need further consideration have been discovered.

- The difference in ATC and NTC must be clarified. The domain for net power injected at an area is not calculated on the same premise for the original model and the model with FBMC, due to unknown NTC values.
- PriMod should be fully scalable, including the implemented flow-based market coupling, and can handle vastly bigger systems. The model needs to be tested with a larger system, preferably with real data, to ensure its accuracy and robustness.
- Development of different GSK-strategies, and comparison between these may provide a greater basis for the decision regarding the optimal strategy.

Flow based market coupling may cause some disruption to the investment in new power plants due to the phenomenon where it operates ”non-intuitive”. Flow-based intuitive market coupling, FBIMC, avoids the occurrences of non-intuitive behaviour of the system, thus ensuring that low priced zones are able to sell to the higher priced. An implementation and comparison between the two flow-based market couplings could be an interesting study.

Bibliography

[1] Bradley, Hax, and Magnanti. *Applied Mathematical Programming*. Addison-Wesley, 1977.

[2] P. J. Burke and A. Abayasekara. The price elasticity of electricity demand in the united states: A three-dimensional analysis. *CAMA Working Paper 50/2017*, 2017.

[3] CWE. Cwe enhanced flow-based mc feasibility report, 2011.

[4] C. Dierstein. Impact of generation shift key determination on flow based market coupling. In *2017 14th International Conference on the European Energy Market (EEM)*, pages 1–7, June 2017.

[5] G. L. Doorman. Hydro power scheduling, 2018.

[6] G. L. Doorman and H. Farahmand. Dc power flow in power markets. In *TET4185, Power Markets, Resources and Environment*, 2018.

[7] EEA. Annex iv - energy, 2019.

[8] EEA. Annex xx - environment, 2019.

[9] ENTSO-E. Net transfer capacities (ntc) and available transfer capacities (atc) in the internal market of electricity in europw (iem). 2000.

[10] EPEX. Core fb mc market design is finalised for implementation. https://www.epexspot.com/en/press-media/press/details/press/Core_FB_MC_Market_Design_is_finalised_for_implementation, 2019.

[11] EU. *A Clean Planet for all A European strategic long-term vision for a prosperous, modern, competitive and climate neutral economy*. 2018.

[12] H. Farahmand. Grid access congestion management. In *TET4185, Power Markets, Resources and Environment*, 2016.

[13] I. Guisández and J. I. Pérez-Díaz. Evaluating approaches for estimating the water value of a hydropower plant in the day-ahead electricity market. In A. Helseth, editor, *Proceedings of the 6th International Workshop on Hydro Scheduling in Competitive Electricity Markets*, pages 8–15, Cham, 2019. Springer International Publishing.

[14] W. E. Hart, C. D. Laird, J.-P. Watson, D. L. Woodruff, G. A. Hackebeil, B. L. Nicholson, and J. D. Siirola. *Pyomo–optimization modeling in python*, volume 67. Springer Science & Business Media, second edition, 2017.

[15] W. E. Hart, J.-P. Watson, and D. L. Woodruff. Pyomo: modeling and solving mathematical programs in python. *Mathematical Programming Computation*, 3(3):219–260, 2011.

[16] L. M. Hatlen and K. K. Aarrestad. Fakta 2015: Energi- og vannressurser i norge, 2015.

[17] E. Haugom, G. A. Hoff, P. Molnr, M. Mortensen, and S. Westgaard. The forward premium in the nord pool power market. *Emerging Markets Finance and Trade*, 54(8):1793–1807, 2018.

[18] A. Helseth. Pribas pricing balancing services in the future nordic power market. https://www.sintef.no/en/projects/pribas-pricing-balancing-services-in-the-future-no/, 2017.

[19] A. Helseth, M. Haugen, S. Jaehnert, B. Mo, H. Farahmand, and C. Naversen. Multi-market price forecasting in hydro-thermal power systems. In *2018 15th International Conference on the European Energy Market (EEM)*, pages 1–5. IEEE, 2018.

[20] A. Helseth, B. Mo, A. Lote Henden, and G. Warland. Detailed long-term hydro-thermal scheduling for expansion planning in the nordic power system. *IET Generation, Transmission Distribution*, 12(2):441–447, 2018.

[21] A. Helseth, G. Warland, and B. Mo. A hydrothermal market model for simulation of area prices including detailed network analyses. *International Transactions on Electrical Energy Systems*, 23:1396–1408, 2012.

[22] T. A. Jensen. Flytbasert markedskobling. https://www.statnett.no/for-aktorer-i-kraftbransjen/utvikling-av-kraftsystemet/prosjekter-og-tiltak/flytbasert-markedskobling/, 2019.

[23] D. Merino. Annual report on the results of monitoring the internal electricity and natural gas markets in 2017, 2018.

[24] B. Mo, S. Martino, C. Naversen, G. Aronsen, and O. Rismark. Benchmarking hydro operation by use of a simulator. In A. Helseth, editor,

Proceedings of the 6th International Workshop on Hydro Scheduling in Competitive Electricity Markets, pages 41–51, Cham, 2019. Springer International Publishing.

[25] Nasdaq. Nordic power products. https://business.nasdaq.com/trade/commodities/products/power-derivatives/nordic.html, 2019.

[26] NEXT. Power purchase agreement. https://www.next-kraftwerke.com/knowledge/ppa-power-purchase-agreement, 2019.

[27] NordPool. History. https://www.nordpoolgroup.com/About-us/History/, 2017.

[28] NordPool. Cross-border intraday: Questions & answers, 2018.

[29] NordPool. Bidding areas. https://www.nordpoolgroup.com/the-power-market/Bidding-areas/, 2019.

[30] NordPool. Intraday trading. https://www.nordpoolgroup.com/trading/intraday-trading/, 2019.

[31] NordPool. Price formation. https://www.nordpoolgroup.com/the-power-market/Day-ahead-market/Price-formation/, 2019.

[32] NordREG. Stakeholder consultation document and impact assessment for the capacity calculation methodology proposal for the nordic ccr, 2017.

[33] S. Olivieri. Intraday and xbid at nord pool. 2018.

[34] T. R. Meberg. Specialization project: Flow-based market coupling in simulations of short-term hydro-thermal scheduling, 2018.

[35] P. Schavemaker. Flow-based market coupling. In *TET4185, Power Markets, Resources and Environment*, 2018.

[36] P. Schavemaker and R. J.L. Beune. Flow-based market coupling and bidding zone delimitation: Key ingredients for an efficient capacity allocation in a zonal system. pages 1–6, 05 2013.

[37] D. Spilde, L. E. Hodge, I. H. Magnussen, J. Hole, M. Buvik, and H. Horne. Strømforbruk mot 2040, 2019.

[38] SSB. Electricity statistics 2017. `https://www.ssb.no/energi-og-industri/statistikker/elektrisitet/aar`, 2018.

[39] Statnett. Capacity calculation methodologies explained flow based market coupling (fb) & coordinated net transfer capacity coupling (cntc).

[40] Statnett. Norwegian grid development plan 2017, 2017.

[41] Statnett. Flytbasert markedskobling. `https://www.statnett.no/for-aktorer-i-kraftbransjen/utvikling-av-kraftsystemet/prosjekter-og-tiltak/flytbasert-markedskobling/`, 2018.

[42] Statnett. Roller i balansemarkedene og vilkår for aggregerte bud, 2018.

[43] R. Sverrisson. Liquidity set to rise amid ppa boom. `https://www.montelnews.com/no/story/`

liquidity-set-to-rise-amid-ppa-boom/990340, 2019.

[44] K. Uhlen. Dc power flow and dc opf. In *TET4115 , Electrical Powersystems*. NTNU, Department of Electric Power Engineering, 2010.

[45] V. Vadlamudi. Optimal power flow studies. In *TET4115 , Electrical Powersystems*. NTNU, Department of Electric Power Engineering, 2017.

[46] N. Witkop. Germany sees third weekend of negative prices. https://www.montelnews.com/en/story/germany-sees-third-weekend-of-negative-prices/993002, 2019.

Appendix

Appendix A: PriMod with implementations

The model used in the master's thesis is developed by the researchers at SINTEF Energy Research, affiliated with the PRIBAS project. The simulations of the model was performed with Pyomo. The modeling language is Python-based, open-source for optimization [14] [15]. The model was solved with CPLEX, an optimization solver provided on an academic licence from IBM.

Below, the complete model with the full implementation is presented. The program code is available at Bitbucket for academic purposes, provided authorization from SINTEF.

Indexes:

k	Timesteps
a	System area
c	Cuts
t	Week
r	Reservoir
i	From area
j	To area
n	Market step
p	Segment

Sets:

$\mathcal{A}$	Price areas
$\mathcal{A}_{\mathcal{H}}$	Price areas - Hydro, subset of $\mathcal{A}$
$\mathcal{A}_{\mathcal{T}}$	Price areas - Thermal, subset of $\mathcal{A}$
$\mathcal{T}$	Weeks
$\mathcal{K}_t$	Timesteps in week t
$\mathcal{C}_t$	Cuts in week t
$\mathcal{M}_a$	Market steps per area
$\mathcal{R}_a$	Reservoirs in area a
$\mathcal{R}_a^{reg}$	Regulated reservoir in set a
$\mathcal{R}_r^{pump}$	Pumping reservoir r
$\mathcal{S}_r^{PQ}$	Segments of peacewise linear PQ
$\mathcal{W}_a$	Wind parks in area a

Parameters:

$\mathcal{T}_{i,j}^{cap}$	Transmission capacity line i to j
$\mathcal{T}_{i,j}^{loss}$	Transmission loss from area i to j
$\mathcal{M}_{n,k}^{price}$	Market price market step n, step k
$\mathcal{M}_{n,k}^{Cap}$	Market capacity step n, step k
$a_{i,j}^{area}$	Zonal PTDF-matrix, line i,j, step k, for injection at the zone $area$
$\mathcal{L}_{a,k}$	Aggregated area loads step k
$\mathcal{W}_{a,k}$	Wind production step k
$\mathcal{R}_r^{max}$	Maximum reservoir capacity r
$\mathcal{R}_r^{min}$	Minimum reservoir r
$\mathcal{R}_r^{init}$	Start reservoir r
$\mathcal{R}_r^{max\ byp}$	Maximum bypass reservoir r
$\mathcal{R}_r^{min\ byp}$	Minimum bypass reservoir r
$\mathcal{R}_r^{max\ dis}$	Maximum discharge reservoir r
$\mathcal{R}_r^{min\ dis}$	Minimum discharge reservoir r
$\mathcal{Q}_p^{PQ}$	Discharge volume per PQ-curve segment p
$\eta_{r,p}^{PQ}$	Generation efficiency per PQ segment p
$\mathcal{H}_r^{h/h_0}$	Relative head at r, referred to initial reservoir
$\mathcal{Q}_r^{pump}$	Pump power form reservoir r
$\mathcal{I}_{r,k}^{reg}$	Regulated inflow reservoir r
$\mathcal{I}_{r,k}^{unreg}$	Unregulated inflow reservoir r
β_c	Cut RHS cut c
$\pi_{r,c}$	Cut coefficient reservoir r, cut c
$\mathcal{P}^{tank}$	Tank water cost
$\mathcal{P}^{spill}$	Spillage penalty
$\mathcal{P}^{byp}$	Bypass penalty
$\mathcal{P}^{slack}$	Slack penalty, dumping excess power

Variables:

$t_{i,j,k}$	Transmission from i to j in timestep k, between areas $\in \mathcal{A}$ and $\in \mathcal{A}_{\mathcal{T}}$
$f_{i,j,k}$	Physical flow between areas $\in \mathcal{A}_{\mathcal{H}}$ in timestep k
$m_{n,k}$	Purchase or sale (+/-) in market step area, step k
$x_{r,k}$	Reservoir level reservoir r, step k
$q_{r,k}$	Release from reservoir r, step k
$q^{dis}_{r,p,k}$	Discharge from reservoir r, segment p, step k
$q^{spill}_{r,k}$	Spillage reservoir r, step k
$q^{byp}_{r,k}$	Bypass reservoir r, step k
$q^{pump}_{r,k}$	Pumping reservoir r, step k
$q^{tun}_{r,k}$	Tunneling between reservoirs r, step k
$q^{tank}_{r,k}$	Tanking reservoir r, step k
α	Future profit function
$p^{hydro}_{r,k}$	Production per module/reservoir r, step k
$y^{slack}_{a,k}$	Slack variable, dumping excess power

Optimize

$$min\ \pi = \sum_{k \in \mathcal{K}_t} \sum_{n \in \mathcal{M}_a} \sum_{a \in \mathcal{A}} \Bigg(\mathcal{M}_{n,k}^{price} \cdot m_{n,k} + \sum_{r \in \mathcal{R}_a} \left(q_{r,k}^{byp} \cdot \mathcal{P}^{byp} + q_{r,k}^{spill} \cdot \mathcal{P}^{spill} + q_{r,k}^{tank} \cdot \mathcal{P}^{tank} + y_{a,k}^{slack} \cdot \mathcal{P}^{slack} \right) \Bigg) + \alpha$$

Subject to:

$$\mathcal{I}_{r,k}^{reg} = x_{r,k} - x_{r,k-1} + q_{r,k} + q_{r,k}^{spill} + q_{r,k}^{pump} - q_{r,k=1}^{tank} - \sum_{r \in \mathcal{R}_{a,\ ups}} \left(q_{r,k}^{spill} + q_{r,k}^{pump} + q_{r,k}^{tun} - q_{r,k}^{tun} + \sum_{p \in \mathcal{S}_r^{PQ}} q_{r,p,k}^{dis} \right)$$

$$\mathcal{I}_{r,k}^{unreg} = q_{r,k}^{byp} - q_{r,k} + \sum_{p \in \mathcal{S}_r^{PQ}} q_{r,p,k}^{dis}$$

$$\mathcal{L}_{a,k} - \mathcal{W}_{a,k} = \sum_{r \in \mathcal{R}_a} \left(\sum_{p \in \mathcal{S}_r^{PQ}} \left(\eta_{r,p}^{PQ} \cdot q_{r,p,k}^{dis} \cdot \mathcal{H}_r^{h/h_0} \right) - \mathcal{Q}_r^{pump} \cdot q_{r,k}^{pump} \right) + \sum_{n \in \mathcal{M}_a} m_{n,k} - \sum_{l \in \mathcal{A}_\mathcal{T}} \left(t_{a,l,k} - t_{l,a,k} \cdot (1 - \mathcal{T}_{l,a}^{loss}) \right) - y_{a,k}^{slack} - \sum_{h \in \mathcal{A}_\mathcal{H}} f_{a,h,k}$$

$$\mathcal{L}_{a,k} - \mathcal{W}_{a,k} = \sum_{n \in \mathcal{M}_a} m_{n,k} - \sum_{j \in \mathcal{A}} t_{a,j,k} - t_{j,a,k} \cdot (1 - \mathcal{T}_{j,a}^{loss})$$

$$f_{i,j,k} = \sum_{a \in \mathcal{A}_\mathcal{H}} a^a_{i,j} \cdot \left(\sum_{h \in \mathcal{A}_\mathcal{H}} f_{a,h,k} + \sum_{l \in \mathcal{A}_\mathcal{T}} t_{a,l,k} - t_{l,a,k} \cdot (1 - \mathcal{T}^{loss}_{l,a}) \right)$$
$$i,\ j \in \mathcal{A}_\mathcal{H}, \quad k \in \mathcal{K}_t$$

$$\alpha + \sum_{a \in \mathcal{A}} \sum_{r \in \mathcal{R}_a} \sum_{c \in \mathcal{C}_t} \pi_{r,c} \cdot x_{r,k} \geq \sum_{c \in \mathcal{C}_t} \beta_c$$

$$-\mathcal{T}^{cap}_{i,j} \leq f_{i,j,k} \leq \mathcal{T}^{cap}_{i,j}, \qquad i,\ j \in \mathcal{A}_\mathcal{H}$$

$$0 \leq t_{i,j,k} \leq \mathcal{T}^{cap}_{i,j}$$

$$\mathcal{R}^{min}_r \leq x_{r,k} \leq \mathcal{R}^{max}_r$$

$$\mathcal{R}^{min\ byp}_r \leq q^{byp}_{r,k} \leq \mathcal{R}^{max\ byp}_r$$

$$\mathcal{R}^{min\ dis}_r \leq \sum_{i \in \mathcal{S}^{PQ}_r} q^{dis}_{r,p,k} \leq \mathcal{R}^{max\ dis}_r$$

$$p^{hydro}_{r,k} = \sum_{p \in \mathcal{S}^{PQ}_r} \eta^{PQ}_{r,p} \cdot q^{dis}_{r,p,k} \cdot \mathcal{H}^{h/h_0}_r$$